https://doi.org/10.5194/egusphere-2026-2849
Preprint. Discussion started: 12 June 2026

Modelling and Interpreting Thermal Stability Indices to Understand Soil Carbon Stabilization Using Soil Properties Data

Kingsley John*[1], Travis Pennell[1,2], Louis-Pierre Comeau[2], Derek H. Lynch[1], Moazame Mesgar[3], Adam W Gillespie[3], Brandon Heung[1]

[1]Department of Plant, Food, and Environmental Science, Dalhousie University, Truro, NS, Canada

[2]Fredericton Research and Development Center, Agriculture and Agri-Food Canada, Fredericton, NB, Canada

[3]School of Environmental Sciences, University of Guelph, Guelph, Ontario, Canada

*Corresponding Author: **Kingsley John*[1]**(john.kingsley@dal.ca**)**

https://doi.org/10.5194/egusphere-2026-2849
Preprint. Discussion started: 12 June 2026

ABSTRACT

Soil organic carbon (SOC) sequestration and nutrient cycling are related to the susceptibility of soil organic matter to biological decomposition. Several studies have demonstrated associations between biological stability and thermal stability, as assessed using programmed pyrolysis. We sought to develop parsimonious machine learning (ML) models to predict SOC stability indices from measured soil properties. The study analyzed indices such as S_1, S_2, and S_3; the oxygen index (OI); the hydrogen index (HI); and T_{50}, which reflect SOC composition, thermal behaviour, and stability. A total of 203 soil samples collected at 0–15cm depth increments from agricultural, forest, and wetland landscapes in New Brunswick, Canada, were analyzed. Feature selection techniques optimized predictive models, and a random forest (RF) was used to develop one. Correlation results revealed that HI was negatively associated with pH (r = –0.35) and bulk density (r = –0.33), whereas OI showed a positive correlation with pH (r = 0.34). Thermal indices were more strongly related to soil chemistry and texture, with S_1 closely correlated with total carbon (r = 0.88) and nitrogen, and S_2 negatively associated with sand (r = –0.66) but positively associated with clay (r = 0.24) and POXC (r = 0.84). T_{50} showed positive correlations with both pH (r = 0.48) and bulk density (r = 0.36), indicating greater thermal stability in higher-pH, compacted soils, though these patterns varied by land use. Random Forest (RF) model predicted S_1-S_3 indices with high accuracy (CCC = 0.83–0.86), while HI and OI were more difficult to model (CCC = 0.44–0.48), suggesting missing biological or environmental predictors; NH_4^+ and POXC emerged as key predictors. Structural equation modeling (SEM), after addressing multicollinearity, supported a hypothesis-driven model that explained ~54% of T_{50} variation. Clay dissolved organic carbon, pH, and aluminum showed significant direct associations with T_{50} (β for pH = 0.44), whereas bulk density showed no meaningful relationship. Our study demonstrates that ML and SEM can reveal patterns and associations between soil properties and thermal stability indices, offering insight into understanding the SOC stability under a changing climate as well as presenting a framework for rapid estimation of SOC stability proxies.

Keywords: Carbon Stabilization; Machine Learning; Geochemical Indicators; Thermal Stability; Rock-Eval Pyrolysis; Structural Equation Model

https://doi.org/10.5194/egusphere-2026-2849
Preprint. Discussion started: 12 June 2026

1. INTRODUCTION

Understanding soil organic carbon (SOC) stability is essential for maintaining the global nutrient cycle and advancing climate-smart agricultural practices (Barreto et al., 2021). SOC stability is referred to as the capacity of organic matter to resist microbial decomposition (Gregorich et al., 2015) and directly influences nutrient cycling, greenhouse gas emissions, and carbon sequestration. The decomposability of SOC, measured as the mineralized carbon per unit of total SOC, is influenced by environmental factors, soil type, microbial activity, and interactions between organic matter and soil minerals (Gregorich et al., 2015).

Thermal analysis is a widely used method for assessing SOC stability, involving controlled heating of soil samples to measure mass loss and energy exchange associated with decomposition of organic bonds and organo-mineral associations (Gillespie et al., 2014; Peltre et al., 2013; Plante et al., 2009). Programmed pyrolysis (PP), as implemented in Rock-Eval or HAWK analyzers (Wildcat Technologies, Humble, Texas, USA), operates by heating whole soil under an inert atmosphere, generating diagnostic indices including S_1 (volatile hydrocarbons), S_2 (hydrocarbons from thermal cracking of non-volatile OM), S_3 (CO_2 from oxygen-containing functional groups), and the derived hydrogen index (HI = S_2/TOC) and oxygen index (OI = S_3/TOC) are commonly used Rock-Eval–derived indicators of organic matter composition (Gillespie et al., 2014; Mesgar et al., 2024b; Plante et al., 2009). Additional thermal stability metrics include T_{50}, the temperature at which 50% of SOC is volatilized (Cécillon et al., 2018; Delahaie et al., 2023). Other thermal analytical approaches, such as thermogravimetry (TG), differential scanning calorimetry (DSC; Gill et al., 2010; McElhaney, 1982), and evolved gas analysis (EGA; Fernández et al., 2011; Risoluti et al., 2022; Verchovsky et al., 2020; Barros et al., 2011; Lorenz et al., 2024), provide complementary information on mass-loss patterns, energy fluxes, and evolved gas composition. Pyrolysis–gas chromatography/mass spectrometry (Py-GC/MS) further enables molecular-level characterization of organic compounds (Fernández et al., 2012; Rombolà et al., 2016). Although these techniques operate on different principles and platforms, integrating their outputs can provide a more complete assessment of SOC composition and persistence (Doležalová-Weissmannová et al., 2023; Gao et al., 2015; Kučerík et al., 2013; Plante et al., 2009).

Previous studies demonstrated that SOC thermal stability was correlated with biological stability, supporting the deployment of thermal analysis as a proxy for decomposability (Gregorich et al., 2015; Peltre et al., 2013). Furthermore, recent studies have linked thermal stability indices to landscape position, management practices, and soil properties; for example, Shi et al. (2024) showed that SOC

https://doi.org/10.5194/egusphere-2026-2849
Preprint. Discussion started: 12 June 2026

thermal stability was higher in depositional landscapes, in comparison to eroded ones, due to the increased clay and silt contents, cation exchange capacity (CEC), and specific surface area. An et al. (2023) found higher thermal stability in hedgerow croplands than adjacent forested areas, suggesting management-induced changes in organo-mineral associations. In permafrost regions, Fang et al. (2021) observed that drier conditions promoted stronger SOC stability via enhanced mineral-organic associations. Collectively, these studies indicate that soil physicochemical properties, specifically texture, mineralogy, and nutrients, are closely linked to the thermal behaviour of SOC.

Despite these advances, no studies have sought to systematically understand the relationships between routinely measured soil properties and thermal stability indices. Traditional methods for assessing SOC stability (e.g., PP, Py-GC/MS, NMR) remain labour-intensive and costly, limiting their application in large-scale monitoring. Pedotransfer functions (PTFs), predictive models estimating hard-to-measure properties from readily available data, offer a potential solution. Originally developed for soil physical properties (Bouma, 1989), PTFs have been extended using machine learning (ML) algorithms such as Random Forest, Cubist, and support vector regression to capture nonlinear relationships between soil properties (Arbor et al., 2023, 2024; Laurence et al., 2023; Padarian et al., 2020; Van Looy et al., 2017). Although PTFs are typically used for predictive purposes, their structure also provides insight into the soil relationships themselves. For example, interpretable ML frameworks, incorporating feature selection (e.g., recursive feature elimination) and *post-hoc* analyses (e.g., variable importance, partial dependence plots) have been advocated to both predict and understand soil-environment relationships (Kasraei et al., 2024; Laurence et al., 2024; Paul et al., 2023; Wadoux & Molnar, 2022). These approaches are highly applicable to developing PTFs for SOC thermal stability while simultaneously elucidating the underlying drivers.

Structural equation modeling (SEM) provides a complementary framework to machine learning by enabling explicit hypothesis testing of theory-derived pathways linking soil properties to thermal stability indices. Unlike black-box prediction algorithms, SEM allows the specification and evaluation of hypothesized relationships among variables, the distinction between direct and indirect associations, and the identification of potential mediation patterns (Grace et al., 2016; Shipley, 2016). This capability is particularly important for understanding how soil properties may interrelate in an integrated system; for example, whether clay content shows a direct association with T_{50}, or whether its relationship with T_{50} is mediated through carbon quality and nutrient availability. Recent studies have demonstrated SEM's utility in revealing complex biogeochemical patterns, including the pathways by which land use

https://doi.org/10.5194/egusphere-2026-2849
Preprint. Discussion started: 12 June 2026

change relates to organic matter stability (Li et al., 2022) and how mineralogical controls correlate with carbon persistence across climatic gradients (Rasmussen et al., 2018). However, no study has systematically integrated SEM with interpretable machine learning to both predict thermal stability indices and explore their multivariate relationships with soil physicochemical properties.

Here, we employ a two-stage analytical framework: first, random forest modelling with recursive feature elimination to identify key predictors and quantify their importance; second, using SEM to test *a priori* hypotheses about causal pathways linking these predictors to T_{50}. This integrated approach goes beyond single-method studies by leveraging machine learning for predictive accuracy and SEM for mechanistic inference, thereby addressing both practical prediction needs and fundamental understanding of SOC stabilization processes.

We hypothesize that soil physical and chemical properties, as key controls on stabilization mechanisms such as organo-mineral association, aggregation, and organic matter chemistry, can serve as proxies for predicting SOC thermal stability indices. Specifically, we expect that soil properties associated with mineral reactivity (clay content, Fe/Al oxides), chemical characteristics (pH, CEC), and labile carbon pools (permanganate oxidizable carbon, dissolved organic carbon) will be significant predictors. Our objectives were as follows: (1) to develop parsimonious machine learning (ML) models to predict a suite of thermal stability indices (S_1, S_2, S_3, HI, OI, and T_{50}) from routinely measured soil properties; (2) to identify the most influential predictors using feature selection and variable importance analysis; and (3) to explore causal pathways linking soil properties to thermal stability using SEM. By leveraging interpretable ML, this study aimed to advance mechanistic understanding of how soil properties inform SOC thermal stability patterns and provide a framework for rapid, low-cost estimation of HAWK pyrolysis thermal stability indices, which explain SOC stability.

2. MATERIALS & METHODS

2.1. Study Area

This research was conducted in the Province of New Brunswick, in the Atlantic Maritime Ecozone of Eastern Canada (**Fig. 1**). The province of 71,388 km^2 receives an annual average precipitation of 1100 mm. Geomorphological features include mountainous regions in the North, lowlands and ocean coasts in the East, and the Saint John River in the South, flowing towards the Bay of Fundy (Pronk and Ruitenberg, 1991). Geological deposits comprise mainly glacial till, glaciofluvial, glaciolacustrine, and glaciomarine deposits (Furze and Arp, 2020; Rampton, 1984). In addition, the area is characterized by outcrops and relatively shallow soils (< 25 cm) across an extended region of the province (Furze et al.,

https://doi.org/10.5194/egusphere-2026-2849
Preprint. Discussion started: 12 June 2026

141 2021). The soils of the region are predominantly Podzols, Gleysols, Cambisols, Luvisols, and Organics
142 with variable degrees of drainage (Fahmy et al., 2010; IUSS Working Group WRB, 2007).

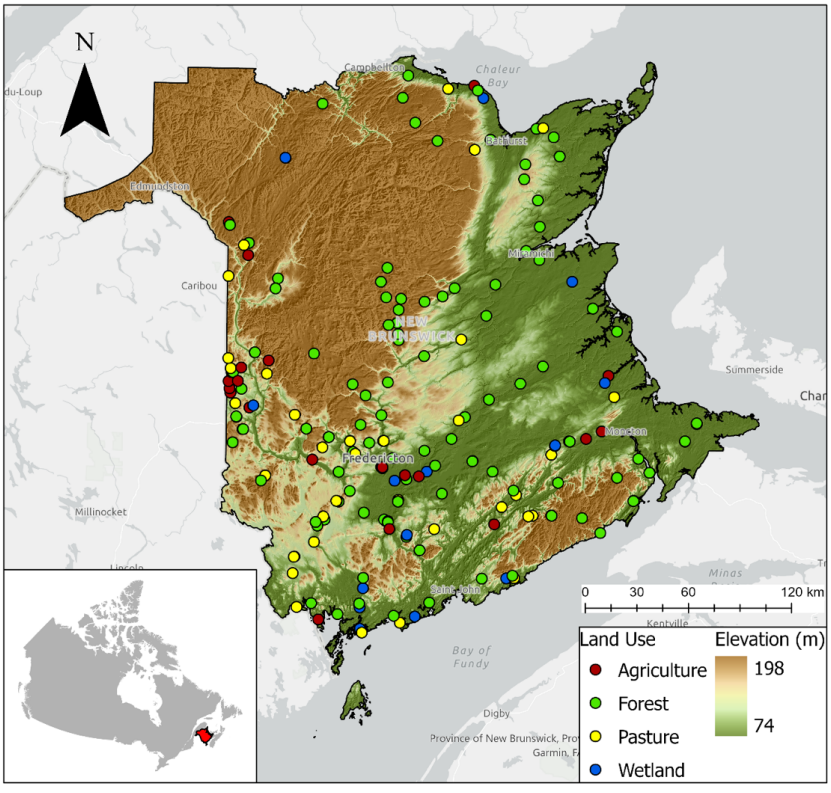

143
144 **Figure 1.** Map of the study area showing soil sampling locations across different land cover types.
145

146 **2.2. Soil Data Acquisition**

147 2.2.1. Soil Sampling Campaign

148 We collected $n = 203$ soil samples at a depth of 0–15 cm via stratified random sampling throughout New
149 Brunswick, representing various land cover types, including agricultural, forested, and wetland areas, as
150 part of the Canadian Soil Biodiversity Observatory program
151 (https://sis.agr.gc.ca/cansis/biome/index.html). Soil samples were transported to the laboratory, air-
152 dried, sieved with a 2 mm sieve, and carefully prepared for analyzing soil properties and carrying out
153 programmed pyrolysis.

154 The primary source of soil data was acquired through an ongoing Agriculture and Agrifood
155 Canada sampling effort. The sampling strategies for this project were a combination of conditioned Latin

https://doi.org/10.5194/egusphere-2026-2849
Preprint. Discussion started: 12 June 2026

hypercube sampling (cLHS; Minasny and McBratney, 2006) and opportunistic sampling. For the cLHS approach, locations were restricted to selected areas that fell within a 200 m buffer of the road for ease of sampling. Opportunistic sampling locations were selected at the discretion of field technicians to supplement cLHS points, ensuring that each sampling point maintained a minimum distance of 10 km between points with a shared land cover classification.

2.2.2. Soil Physical and Chemical Properties

All laboratory analysis methods were determined using standard soil testing protocols as reported in Vallotton et al. (2025). These included sand, silt, clay (particle size fractions, %); BD (bulk density, g cm^{-3}) and BD_FINE (bulk density corrected for coarse fragments, g cm^{-3}); and Agg_stab (aggregate stability, %) at 0 -15cm. Soil carbon and nitrogen pools comprised: TC (total carbon, %), TN (total nitrogen, %), and C:N (carbon-to-nitrogen ratio); POXC (permanganate oxidizable carbon, mg kg^{-1}), a measure of labile carbon; DOC (dissolved organic carbon, ppm); TDN (total dissolved nitrogen, ppm); TON (total organic nitrogen, ppm); TIN (total inorganic nitrogen, ppm); NH_4^+ (ammonium-nitrogen, ppm); and NO_3^- (nitrate-nitrogen, ppm). Soil chemical properties and nutrients included: pH (soil pH); CEC (cation exchange capacity, meq 100 g^{-1}); Base_sat (base saturation, %); P_2O_5 (phosphate, ppm); K_2O (potash, ppm); and extractable nutrients B (boron), Cu (copper), Zn (zinc), S (sulfur), Mg (magnesium), Fe (iron), Ca (calcium), Mn (manganese), Al (aluminum), and Na (sodium), all in ppm. Exchangeable cation saturations were expressed as percentages: K_sat (potassium saturation), Mg_sat (magnesium saturation), Ca_sat (calcium saturation), H_sat (hydrogen saturation), and Na_sat (sodium saturation).

2.2.3. Thermal Stability Indicators

SOC thermal stability was assessed using programmed pyrolysis (PP), as described by Mesgar et al. (2024). Analyses were performed using a HAWK pyrolysis instrument (Wildcat Technologies, Humble, Texas, USA) at the Geological Survey of Canada, Calgary. This approach is analogous to Rock-Eval© pyrolysis, involving two controlled heating stages under anaerobic (pyrolysis) and oxidative conditions.

In the initial pyrolysis phase, 70 mg of finely ground (< 250 µm) soil was held isothermally under N_2 at 300 °C for 3 min. During this stage, the hydrocarbons (HC) released were detected using a Flame Ionization Detector (FID) and recorded as the S_1 peak (mg HC g^{-1} of sample). Following the SI step, the temperature was increased at a rate of 20 °C min^{-1} to 650 °C to thermally decompose the more thermally

https://doi.org/10.5194/egusphere-2026-2849
Preprint. Discussion started: 12 June 2026

stable fraction of OM. The HC released in this phase was measured as the S_2 peak (mg HC g^{-1} of sample), also recorded via the FID. Together, S_1 and S_2 represent the organic C liberated during thermal decomposition (Table 1). Concurrently, evolved gases, including carbon dioxide (CO_2) and carbon monoxide (CO), released during pyrolysis were monitored using an infrared (IR) detector and are represented as S3' (mg CO g^{-1} of sample; Baudin et al., 2015; Table 1).

From these measurements, several derived indices were calculated. The Hydrogen Index (HI, mg HC/g TOC) and Oxygen Index (OI, mg O_2/g TOC) are calculated by normalizing the S_2 and S_3 values, respectively, to the TOC content of the sample. The HI reflects the hydrogen-rich, energy-dense portion of SOC and is often used as a proxy for OM quality (Gillespie et al., 2014; Gregorich et al., 2015). The OI characterizes the relative oxygen content in OM and its potential oxidizability. The T_{50} is a thermal stability index denote the temperature at which 50% of the total pyrolyzable organic matter is released. T_{50} captures the median decomposition temperature across the full temperature range (Barros et al., 2011; Gregorich et al., 2015). Higher T_{50} values indicate greater SOC thermal resistance and are typically associated with mineral-associated organic matter or chemically recalcitrant compounds.

Table 1. HAWK Rock-Eval pyrolysis thermal indices

Thermal Indices	Abbreviation	Definitions	Unit
S1	S1	Hydrocarbon[1] released between 0 and 300 °C	HC-mg[1] / g-rock
S2	S2	Hydrocarbon[1] produced between 200 and 650 °C	HC-mg[1] / g-rock
OI	OI	Equal to (S3/TOC[2]) × 100	O_2-mg / g TOC[2]
HI	HI	Equal to ((S1 + S2) / TOC[2]) × 100	HC-mg[1] / g TOC[2]
S3′	S3	Pyrolysis of OM[3]	mg-CO_2 / g-rock
T50	T50	Temperature at which 50% of the loss in SOM[4] weight occurs	Celsius (°C)

[1] HC = hydrocarbons; [2] TOC = total organic carbon; [3] OM = organic matter; [5]SOM = organic matter;

https://doi.org/10.5194/egusphere-2026-2849
Preprint. Discussion started: 12 June 2026

2.3. Predictive Modelling Framework

The predictive modelling framework follows the approach of Kasraei et al. (2024). It involves four key steps: (1) addressing multicollinearity among predictor variables variance inflation factor (VIF) analysis (**Section 2.3.1**); (2) fitting a Random Forest (RF) model to predict each thermal stability index (**Section 2.3.2**); (3) applying recursive feature elimination (RFE) to ensure model parsimony by removing non-informative variables (**Section 2.3.3**); and (4) conducting *post-hoc* model assessments, including structural equation modeling (SEM) and model interpretability techniques (Fig. 2; **Section 2.4**).

2.3.1. Addressing Multicollinearity

Multicollinearity among predictors was assessed and mitigated using the VIF, which quantifies the proportion of variance in each predictor that can be explained by all other predictors (Craney & and Surles, 2002). Here, VIF was calculated in equation (1):

$$VIF_i = \frac{1}{1 - R_i^2} \qquad (1)$$

where r_i^2 is the coefficient of determination from fitting a linear regression between the *i*-th predictor and all other predictors. VIF can range from 1 to infinity, with a value of 1 indicating no multicollinearity, values between 1 and 5 suggesting a moderate collinearity, and values > 5 indicating a high degree of collinearity (Curto & and Pinto, 2011; Thompson et al., 2017). A stepwise approach was used to address multicollinearity by iteratively removing covariates with the highest VIF until all remaining covariates had a VIF of 5 or lower, reducing the full set of covariates to 21 predictors. The VIF analysis was implemented in R using the *oss.seqVIF* function in the *onsoilsurvey* package (Saurette, 2021).

2.3.2. Random Forest

The RF model is an ensemble machine learning algorithm based on decision trees, which was used to model the relationship between soil physicochemical properties and thermal stability indices. For each tree-based model (i.e., base learner), the training data is split at nodes using the values of the predictor variables to maximize within-node similarity and between-node differences (Breiman et al., 1948). RF enhances this approach by constructing multiple trees, each trained on a randomized bootstrap sample (with replacement) of the dataset, creating a diverse 'forest' of decision trees. At each node, a random subset of predictors is selected for splitting. The final RF prediction is determined by aggregating the

https://doi.org/10.5194/egusphere-2026-2849
Preprint. Discussion started: 12 June 2026

outputs of all trees, using averaging for regression applications. Two key hyperparameters define the RF model: n_{tree}, which specifies the number of decision trees, and m_{try}, which sets the maximum number of covariates considered at each split (Breiman, 2001).

Model performance was assessed using Lin's concordance correlation coefficient (CCC), coefficient of determination (R^2), root mean square error (RMSE), and bias. The best-performing model for each index was selected based on the highest CCC and lowest RMSE values. The models were tuned using a predefined grid of hyperparameters, spanning the range of m_{try} values, and using a 10-fold cross-validation procedure with 20 repeats.

2.3.3. Recursive Feature Elimination

During the RF modelling process, the 21 uncorrelated variables identified through VIF were further reduced using RFE to identify the minimal set of variables that maintains model performance. RFE was implemented using the *caretFuncs* function within the *caret* R package, which evaluates the contribution of each predictor against the response variable (e.g., thermal stability indicators) based on variable importance scores. Less important features were progressively removed during the iteration.

Following this, the RFE output provided various features alongside their corresponding performance metrics. Features resulting in the lowest RMSE were selected for modeling (Kuhn, 2019). Additionally, the RMSE from repeated cross-validation runs was used to compute and plot the 90% confidence intervals (CI) for each RFE model. The model with the reduced set of covariates achieving the lowest RMSE was considered the baseline for comparison with other models. Here, the 'smallest' model, where removing an additional predictor would not significantly increase RMSE, was retained and subsequently used to build the models and SEM for thermal stability indices.

2.4. *Post-Hoc* Model Assessment

Several *post-hoc* assessment tools, such as Shapley value, partial dependence plots (PDP), individual conditional expectation (ICE) plots, and accumulated local effects (ALE) plots, have been developed to address the challenge of interpreting ML prediction (Friedman, 2001; Goldstein et al., 2015; Apley and Zhu, 2020; Molnar et al., 2021). This need arises because many ML models are considered 'black box' models. Collectively, the methods help integrate physical knowledge into ML to improve interpretability and transparency.

https://doi.org/10.5194/egusphere-2026-2849
Preprint. Discussion started: 12 June 2026

2.4.1. Variable Importance Analysis

We used the *caret* package in R to generate permutation-based, model-agnostic measures of variable importance for predicting thermal indices using RF. This analysis is important as it allows the model to measure the contribution of each predictor (e.g., soil physical and chemical properties) to overall accuracy.

2.4.2. Partial Dependence Plots & Individual Conditional Expectation Plots

The PDPs show the interaction between the features and the prediction (Friedman, 2001). The PDP estimates the mean marginal effect of predictors on the predicted thermal indices, which can be determined value in regression. To plot these effects, the dataset was first split into two groups: the feature of interest and all other features. Following this, each value from this set was systematically substituted into the feature of interest across all observations. This created a synthetic data point where only the feature of interest varied, while all other features remained unchanged. Lastly, the trained RF learner then predicted the target variable (e.g., thermal index) for each synthetic observation. These predictions represented the marginal effect of the feature of interest.

Unlike PDPs, which show average effects, ICE plots display the relationship between a feature and the predicted response for each observation (Goldstein et al., 2015). Like PDP, ICE keeps all other features constant while systematically varying the feature of interest across a defined grid. For each observation, synthetic data points are created by replacing the original feature value with values from this grid. The model then predicts the response for each of these synthetic instances. Repeating this process for all observations allows ICE plots to reveal how each feature influences individual predictions, offering a more detailed and transparent view of model behavior.

2.4.3. Structural Equation Modelling (SEM)

We employed structural equation modeling (SEM) to test *a priori* hypotheses about theoretically derived relationships between soil properties and thermal stability of SOC (e.g., T_{50}), complementing predictive machine learning with path analysis that can reveal direct and indirect associations. Before the SEM specification, we addressed severe multicollinearity (Section 2.3.1). Following Wade et al. (2026) on the importance of justifiable *a priori* models, we formulated five hypotheses based on biogeochemical theory, predicting specific directional relationships: clay content would yield a positive association with T_{50}, consistent with physical protection mechanisms (H_1; Six et al., 2004); dissolved organic carbon

https://doi.org/10.5194/egusphere-2026-2849
Preprint. Discussion started: 12 June 2026

would yield a negative interaction with T_{50}, reflecting labile carbon pools (H_2; Lehmann & Kleber, 2015); soil pH would demonstrate a positive relationship with T_{50} through cation bridging effects (H_3; Rowley et al., 2018); aluminum content would show a positive interaction with T_{50}, consistent with organo-mineral complex formation (H_4; Kleber et al., 2007); and bulk density would show a positive interaction with T_{50} through physical structure effects (H_5; Dungait et al., 2012).

Using the *lavaan* package (Rosseel, 2012) with standardized variables, we compared three models: the *a priori* hypothesis model (Model 1; T_{50} as a function of clay, dissolved carbon, pH, aluminum, and bulk density); an exploratory model incorporating additional variables (Model 2; permanganate oxidizable carbon, C:N, P_2O_5) that showed strong bivariate correlations ($|r| > 0.30$) with T_{50}; and a mediation model testing indirect pathways of pH and clay via dissolved carbon and aluminum (Model 3). Models were fitted using maximum likelihood with robust standard errors and bootstrap resampling ($n = 1000$) for mediation analysis (Preacher & Hayes, 2008). Model fit was assessed using the Akaike information criterion (AIC), Bayesian information criterion (BIC), comparative fit index (CFI ≥ 0.90), and root mean square error of approximation (RMSEA ≤ 0.08; Hu & Bentler, 1999; Shi et al., 2019). It is important to note that lower AIC values indicate better fit, but significance may depend on sample size; lower BIC values indicate better fit; RMSEA ≤ 0.08 or lower values (acceptable), ≤ 0.05 (good fit); CFI≥ 0.90 (acceptable), ≥ 0.95 (good fit) (Shi et al., 2019).

Model 1 was selected as the primary model based on theoretical grounding, parsimony, and comparable explanatory power to more complex alternatives. Standardized path coefficients (β) were interpreted at $\alpha = 0.05$, with hypotheses considered supported if coefficients were statistically significant and directionally consistent with predictions. We further tested model robustness using 10-fold cross-validation repeated 20 times, with close agreement between calibration and validation (R^2). We present path diagrams generated using *semPlot* (Epskamp et al., 2012) with color-coded edges indicating direction and significance of associations. We explicitly distinguish exploratory Model 2 results from confirmatory hypothesis tests, recognizing that all findings represent correlational evidence consistent with, but not proof of, causal mechanisms (Wade et al., 2026).

https://doi.org/10.5194/egusphere-2026-2849
Preprint. Discussion started: 12 June 2026

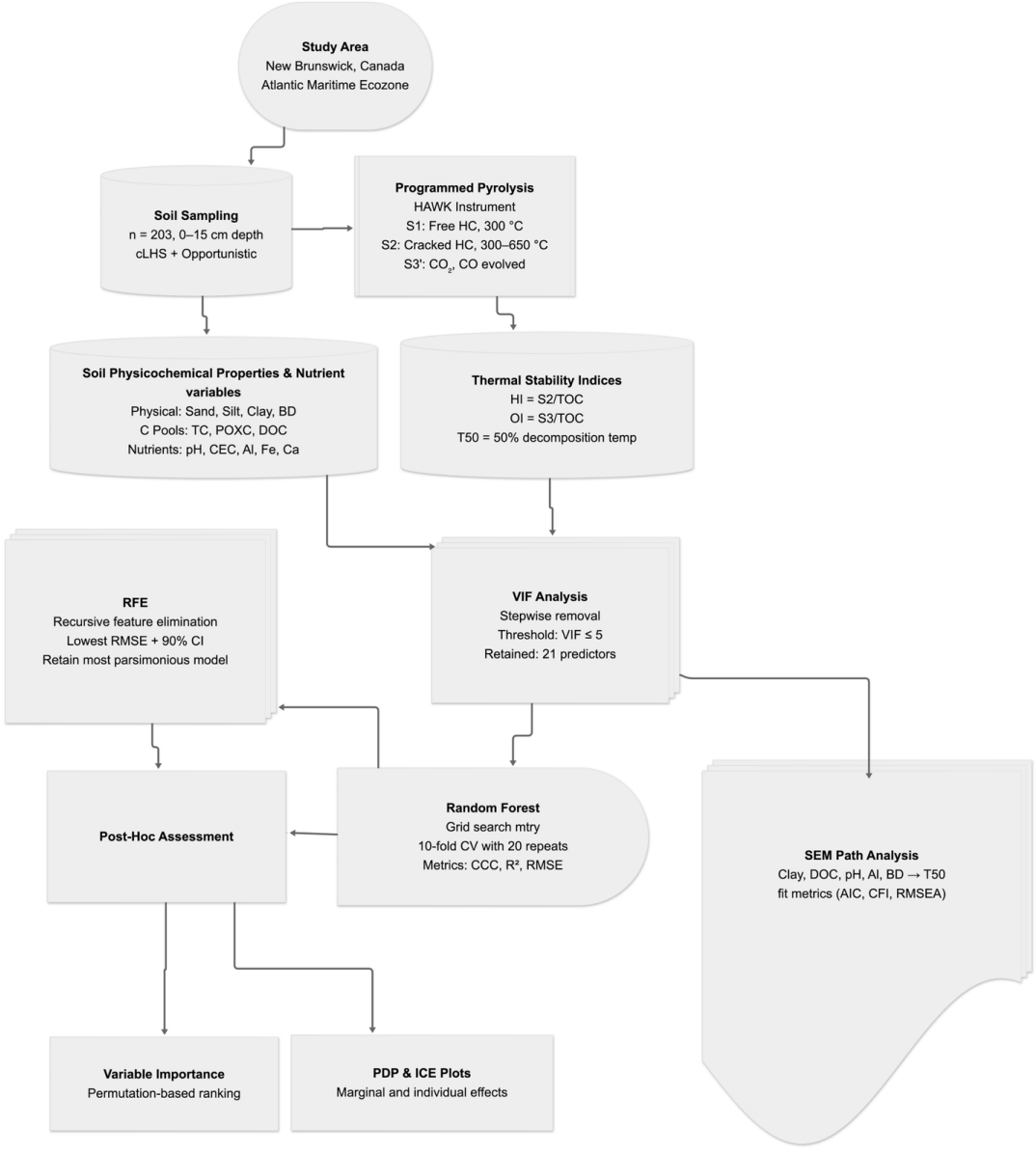

316

317 **Figure 2.** Methodological framework for predicting thermal stability indices using soil physicochemical
318 properties and machine learning (ML) and structural equation model (SEM).

319 **3. RESULTS & DISCUSSION**

320 **3.1. Summary Statistics of Thermal Stability Indices**

https://doi.org/10.5194/egusphere-2026-2849
Preprint. Discussion started: 12 June 2026

Fig. 3 shows the boxplots and cumulative distribution functions (CDFs) for thermal stability indices derived from HAWK-programmed pyrolysis across New Brunswick soils. These indices include volatile hydrocarbons already present (S_1), pyrolysate (S_2), carbon dioxide (S_3), hydrogen index (HI), oxygen index (OI), and T_{50} (temperature at which 50% of OM is pyrolyzed). Here, the result shows that HI and S_2 have broad interquartile ranges, indicating heterogeneity in thermally stable, hydrogen-rich SOC across sample locations (e.g., land uses; Barros et al., 2011; Gillespie et al., 2014). In contrast, the narrower distributions of OI and S_1 suggest greater uniformity in volatile content and oxidation potential, potentially due to more consistent environmental or soil conditions across sites (Gao et al., 2015; Plante et al., 2009). The high median observed in T_{50} (around 350–420 °C) may suggest a significant presence of thermally stable SOC to readily decomposable SOC, which supports past studies indicating that higher pyrolysis temperatures correlate with stable, mineral-associated SOC in complex soils (Fernández et al., 2011, 2012; Kučerík et al., 2013, 2018; Peltre et al., 2013).

In the Supplementary Materials, we present violin boxplots and spatial distribution plots of thermal stability indices obtained from HAWK-programmed pyrolysis across various land use types (Figs. S1-S6). The plots revealed that the forest land use consistently showed higher T_{50} values and moderate-to-high S_2, suggesting greater thermal stability and a higher proportion of recalcitrant SOC, which may be due to the age of vegetation inputs, acidic conditions, and stronger organo-mineral associations that promote stabilization of thermally resistant carbon fractions (Gregorich et al., 2015). Agricultural land use exhibited lower and more varying T_{50} alongside high S_1 and HI, reflecting disturbance from tillage, enhanced mineralization, and a greater contribution of labile, recently derived carbon pools from crop residues and amendments (Gregorich et al., 2015; Gillespie et al., 2014). The wetland ecosystem displayed a high S_2 with variable T_{50}, confirming the accumulation of fresh, plant-derived organic matter under anoxic conditions that limit oxidative decomposition and support carbon sequestration despite lower thermal maturity in certain fractions (Gregorich et al., 2015). Pastures presented intermediate spatial distribution, with moderate T_{50} and HI influenced by perennial plant root inputs, grazing effects, and partial mineral protection mechanisms that stabilize organic matter to a degree between forest and cropland systems.

https://doi.org/10.5194/egusphere-2026-2849
Preprint. Discussion started: 12 June 2026

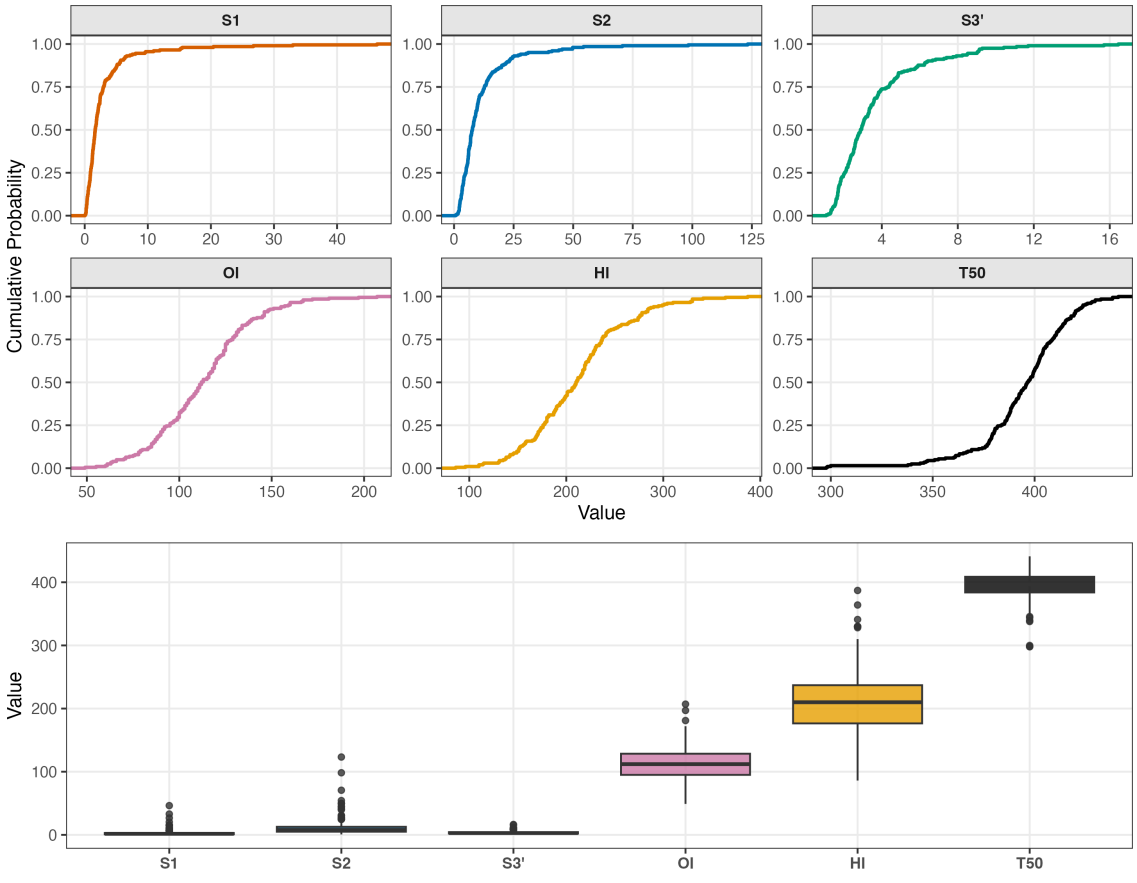

Figure 3. Cumulative distribution function (CDF) plots (top) and boxplots (bottom) for thermal stability indices derived from HAWK-Programmed Pyrolysis. The indices include the S_1, S_2, S_3, OI, HI, and T_{50}, which provide insights into the thermal degradation of SOC.

3.2. Relationships between Thermal Stability and Physicochemical Properties of Soil

3.2.1. S_1

A negative correlation with soil pH ($r = -0.33$) suggested that higher free hydrocarbon content is associated with more acidic soils (Fig. 4). Strong positive correlations with total nitrogen (TN; $r = 0.64$) and %C ($r = 0.88$) indicate that elevated S_1 values correspond to nutrient-rich environments. Additional positive correlations with clay ($r = 0.38$), C:N ($r = 0.53$), POXC ($r = 0.70$), DOC ($r = 0.85$), TDN ($r = 0.31$), NH_4^+ ($r = 0.58$), TON ($r = 0.21$), and CEC ($r = 0.40$) reinforce the association between S_1, labile

https://doi.org/10.5194/egusphere-2026-2849
Preprint. Discussion started: 12 June 2026

carbon pools, and overall soil fertility. Collectively, these relationships highlight how free hydrocarbons in SOM reflect interactions among soil acidity, nutrient availability, and physical protection mechanisms (Berthrong et al., 2009, 2012).

3.2.2. S_2

S_2 was significantly correlated with various soil physicochemical properties reflecting its link to kerogen-like, thermally labile hydrocarbons in SOM (Fig. 4). A moderate negative correlation with soil pH ($r = -0.29$) suggests that acidic soils, where decomposition proceeds more slowly, tend to accumulate more S_2-related organic matter (Disnar et al., 2003). The strong negative correlation with sand ($r = -0.25$) indicates that finer-textured soils protect organic matter and thus have higher S_2 values, consistent with lower retention and stabilization capacities in sandy soils (Entio et al., 2024; Schmidt et al., 2011; Six & Paustian, 2014). Strong positive correlations were observed between S_2 and TN ($r = 0.74$), TC ($r = 0.92$), POXC ($r = 0.77$), DOC ($r = 0.81$), NH_4^+ ($r = 0.49$), clay ($r = 0.41$), Zn ($r = 0.42$) and TIN ($r = 0.31$), indicating that S_2 tracks nutrient-rich carbon fractions associated with soil fertility (Culman et al., 2012).

In contrast, negative correlations with BD ($r = -0.57$), Al ($r = -0.34$), K_sat ($r = -0.22$), and Mg_sat ($r = -0.21$) suggest that BD soils and metal-rich environments, often associated with higher temperatures during the S_2 pyrolysis phase (650 °C) and may not favor the accumulation of kerogen-like material. This aligns with evidence that high BD and elevated soil temperatures promote SOM mineralization (Davidson & Janssens, 2006; Disnar et al., 2003).

3.2.3 S_3

The indicator S_3 exhibited a positive correlation with fine-textured and chemically reactive soil components, such as clay ($r = 0.30$) and silt ($r = 0.32$). This suggests that particle size fractions play a crucial role in protecting the release of CO_2 from organic matter. Conversely, S_3 had a negative relationship with sand fractions ($r = -0.38$) and BD ($r = -0.52$), indicating a higher CO_2 release in coarse-textured soils. Among chemical properties, S_3 correlated positively with CEC ($r \approx 0.56$), TC ($r \approx 0.86$), TN ($r = 0.90$), POXC ($r = 0.84$), and DOC ($r = 0.52$). This highlights that S_3 increases with organic matter content, and soils dominated by readily oxidizable carbon tend to accumulate less thermally stable material. Overall, these patterns suggest that S_3 was likely influenced by the type of organic matter formation in the soil, driven by fine texture, CEC, and labile carbon dynamics (Mesgar et al., 2024b).

https://doi.org/10.5194/egusphere-2026-2849
Preprint. Discussion started: 12 June 2026

3.2.4. Oxygen Index (OI)

OI showed a positive correlation with soil pH (r = 0.34), indicating that higher OI values correspond to higher pH. This suggests that neutral to alkaline conditions may favor oxidative transformations of SOC (Wenyika et al., 2025). The negative correlation between OI and C:N (r = −0.35) implies that increases were possibly associated with decreases in C:N, which could reflect greater nitrogen availability and enhanced microbial decomposition that promotes nutrient cycling and the accumulation of more oxidized residues (Cotrufo et al., 2013, 2022). However, these patterns contrasted with our study, in which lower C:N ratios (indicating higher nitrogen content and greater organic matter quality) were more often associated with higher HI and lower OI values. Higher nitrogen availability is typically linked to enrichment in labile, hydrogen-rich components such as O-alkyl-C and peptides, which contribute to elevated HI rather than OI (Mesgar et al., 2024b). The observed positive relationship between OI and lower C:N in this study may therefore be site-specific, potentially driven by land-use differences; for example, croplands often exhibit lower C:N and higher OI due to accelerated oxidative processing (Gillespie et al., 2014) or site-specific interactions in New Brunswick's soils. A positive correlation between OI and Al (r = 0.30) further suggests that aluminum-rich soils may exhibit greater oxidative signatures, likely due to organo-mineral interactions that influence SOM stabilization and transformation pathways (Mesgar et al., 2024a; Mayer et al., 2023; Sparks, 1995; Wagai & Mayer, 2007).

3.2.5. Hydrogen Index (HI)

In Fig. 4, HI showed a negative correlation with BD (r = −0.38), pH (r = −0.34), and Al (r = −0.33). This suggests that decreases in BD, pH, and Al levels were possibly associated with increases in HI. High HI is often characterized by less stable SOC or rapidly decomposable and unstable SOC, which may control BD variation (Yu et al., 2020). This result suggests that soils with higher compaction tend to contain SOC with lower hydrogen. This pattern may reflect reduced inputs of fresh, O-alkyl-C-rich organic matter and/or advanced decomposition under conditions of limited organic inputs. Increased bulk density is also associated with altered aggregation and mineral protection mechanisms, which can influence SOC composition and apparent stability rather than directly enhancing decomposability (Yu et al., 2020).

In contrast, HI showed a positive correlation with TC (r = 0.40), TN (r = 0.30), POXC (r = 0.30), and DOC (r = 0.36), reflecting the role of labile carbon fractions in supporting microbial activity, which may in turn enhance HI (Kögel-Knabner, 2002). It is important to note that HI reflects the chemical

https://doi.org/10.5194/egusphere-2026-2849
Preprint. Discussion started: 12 June 2026

composition of SOC; higher HI content generally indicates a greater proportion of hydrogen-rich, labile components, such as aliphatic and O-alkyl-C functional groups. In contrast, soils with high SOC can still exhibit low HI if their carbon is dominated by condensed aromatic structures, which are hydrogen-poor and therefore do not contribute to elevated HI values (Moore et al., 2017).

A negative correlation between HI and Al ($r = -0.33$) suggests that Al complexes are associated with organic matter of lower hydrogen richness, reflecting differences in molecular composition rather than lower organic matter content. In contrast, the positive correlation with cation exchange capacity (CEC; $r = 0.27$) suggests that organic matter composition, particularly the presence of labile functional groups, may enhance the retention of exchangeable cations.

3.2.6. T_{50}

We observed a positive correlation between T_{50} and soil pH ($r = 0.48$), which suggests that more thermally stable SOC was prevalent in alkaline soils, likely due to reduced microbial decomposition rates under higher pH conditions, which promote SOC preservation (Almagro et al., 2021; Disnar et al., 2003; Solomon et al., 2012; Tao et al., 2023). However, we also noted that acidic soils could show strong SOC stability due to the presence of Fe and Al, which form strong organo-mineral bonds with organic matter, resulting in higher T_{50} values. Similarly, the positive correlation with BD ($r = 0.36$) indicates that compacted soils tend to contain more thermally stable SOC, potentially because reduced pore space limits microbial access to organic substrates, favoring the accumulation of recalcitrant carbon fractions (Six et al., 2002).

Conversely, T_{50} showed negative correlations with TC ($r = -0.46$) and C:N ($r = -0.58$), suggesting that soils richer in labile SOC tend to have lower T_{50} values. Strong negative correlations with DOC ($r = -0.60$) and POXC ($r = -0.43$) further support this trend, implying that high T_{50} values are associated with soils containing fewer readily decomposable SOC pools, likely due to the preferential breakdown of easily accessible organic compounds (Barreto et al., 2021; Briedis et al., 2023; Liu et al., 2020). Additionally, the negative correlations with NH_4 ($r = -0.28$) and CEC ($r = -0.44$) suggest that soils with higher T_{50} values yield a large proportion of recalcitrant SOC that has undergone advanced decomposition and releases its labile constituents (Cremer & Prietzel, 2017; Rakhsh et al., 2017).

In contrast, T_{50} showed a positive correlation with P_2O_5 ($r = 0.33$), K_sat ($r = 0.33$), Mg_sat ($r = 0.33$), Ca_sat ($r = 0.34$), and base_sat ($r = 0.36$), respectively. This is likely due to stabilization mechanisms involving metal oxides and clay minerals, which protect SOC from microbial degradation

https://doi.org/10.5194/egusphere-2026-2849
Preprint. Discussion started: 12 June 2026

(Wagai & Mayer, 2007). Additionally, the negative correlation with % H ($r = -0.36$) indicates that more thermally stable organic matter has a lower hydrogen content, consistent with advanced decomposition and oxidation processes that remove hydrogen-rich aliphatic compounds (Cecillon et al., 2018; Gregorich et al., 2015; Li et al., 2020; Sebag et al., 2016). These findings highlight the complex interactions between thermal stability, soil nutrient availability, and metal oxides, aligning with the observations of Lehmann & Kleber (2015).

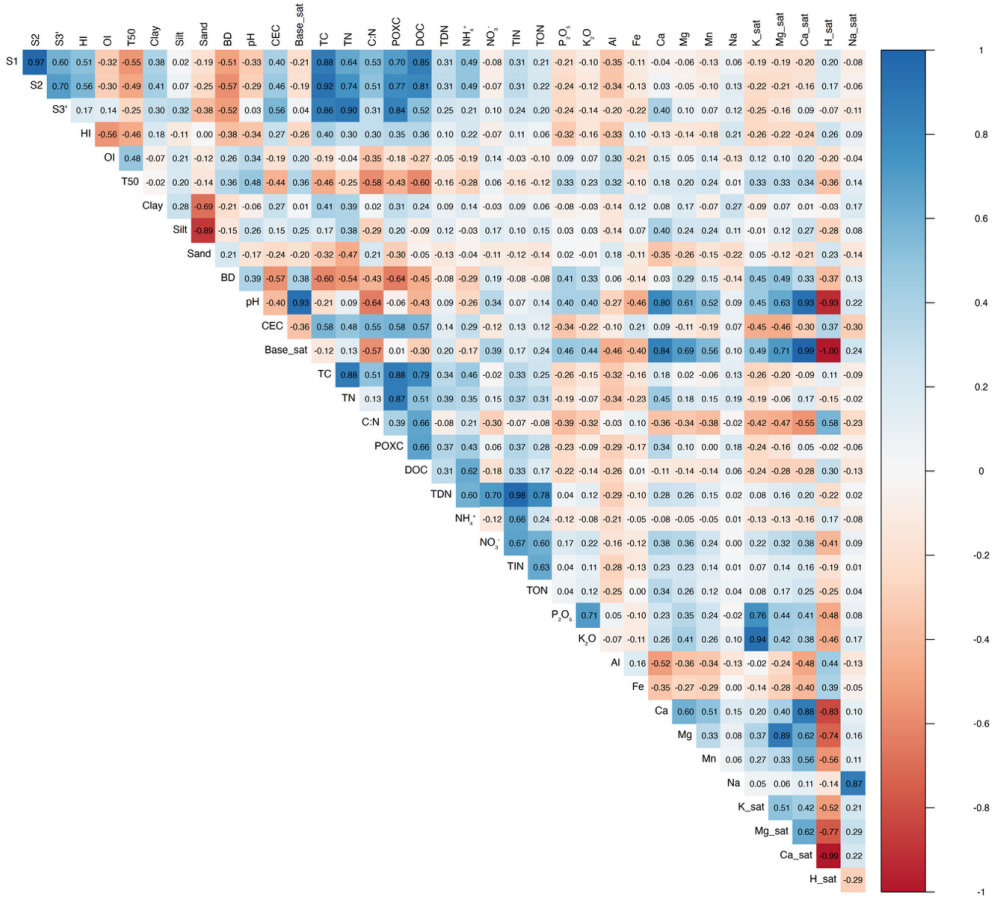

Figure 4. Correlation matrix between thermal stability indices and soil properties.

3.3. Predictions of Thermal Stability Indices using Random Forest Learner

Using the minimum number of covariates identified by RFE, we developed predictive models for each thermal stability index (S_1, S_2, S_3', OI, HI, and T_{50}; see Fig. 5). Accuracy metrics are presented in Table 2, and model residual scatterplots in Fig. 5. The models for S_1, S_2, S_3', OI, HI, and T_{50} showed the highest

https://doi.org/10.5194/egusphere-2026-2849
Preprint. Discussion started: 12 June 2026

accuracy, as reflected by their high CCC values (>0.80), low RMSE, and bias, suggesting model consistency in capturing variations in SOC stability using thermal stability indicators and soil properties. In contrast, HI and OI had the lowest model performance (CCC ≤ 0.48). Additionally, T_{50} showed moderate accuracy, with CCC values ranging from 0.58 to 0.66. While these models provided important insights into SOC stability, they also suggested that incorporating additional variables, such as biological, climatic, and land use factors, could enhance predictive capabilities. These results corroborate previous studies on SOC dynamics and stabilization, where active or readily decomposable SOC fractions, mineral interactions, and soil structure are known to significantly influence carbon cycling, persistence, and storage in soils (Lal, 2004; Wiesmeier et al., 2019).

3.3.1. S_1 *Model*

The S_1 model yielded higher accuracy metrics with a CCC of 0.85 and a low RMSE of 1.19 HC-mg/g-rock compared to both HI and OI (Table 2 and Fig. 5). The scatterplot for S_1 showed that the regression line was close to 1:1, indicating a better model was obtained using the selected predictors. In addition, Fig. 6 shows the variable importance plot of the S_1 model with POXC as the most important predictor with the highest importance score (> 90%), indicating that labile organic carbon strongly controls S_1. This was closely followed by DOC, which yielded an importance score of 85%, indicating that SOC stabilizes via mineral interactions and contributes to S_1 variability. Also, it may be possible that at the S_1 temperature level, partially transformed hydrocarbon compounds become volatilized and hence contribute to the variability of S_1 as an index in understanding the stability of C in soils. BD had a variable importance of 32%, likely due to its effect on microbial access to oxygen, which impacted SOC decomposition (Tao et al., 2023). CEC contributed 28% of the relative importance, suggesting that clay–mineral interactions play a moderate role in thermal indices prediction. The CEC's moderate contribution can vary depending on the type of clay present in the soil (Ma et al., 2024). Conversely, the C:N had an importance of 24%, indicating that, compared with other predictors in the model, it played a moderate role in distinguishing patterns potentially linked to nitrogen availability and the accumulation of more labile carbon. The result highlights that readily decomposable C has a relationship with the S_1 index, while BD and other soil properties play a secondary role in stabilizing SOC.

Fig. 7 presents PDP and ICE plots for S_1 model predictions. In the S_1 model, DOC and POXC showed a strong positive correlation, suggesting their significant role in hydrocarbon (HC) release below 300°C, aligning with Leifeld et al. (2002) da Silva et al. (2025). Conversely, BD exhibited a declining

https://doi.org/10.5194/egusphere-2026-2849
Preprint. Discussion started: 12 June 2026

trend, indicating that compacted soil restricts microbial access to organic material, thereby stabilizing SOC and limiting labile carbon availability (Six et al., 2004; Six & Paustian, 2014). CEC and C:N displayed stable trends with slight increases, implying contributions from soil mineral interactions and nitrogen content.

3.3.2. S_2 *Model*

The S_2 model demonstrated high predictive accuracy with a CCC of 0.86 and RMSE of 4.01 HC-mg/g-rock (Table 2 and Fig. 5). The scatterplot showed close alignment between predicted and observed values, with the regression line approximating the 1:1 line. Variable importance analysis (Fig. 6) revealed that POXC was the dominant predictor, followed by DOC, BD, CEC, and C:N. This indicates that S_2, which is hydrocarbons from thermal cracking of non-volatile organic matter, is strongly associated with labile carbon pools and soil physical properties.

Partial dependence plots (Fig. 7) showed that POXC had a strong positive relationship with predicted S_2 values, confirming that readily available carbon pools drive the formation of kerogen-like hydrocarbons. Conversely, BD exhibited a consistent negative trend, suggesting that soil compaction limits the accumulation or detection of these thermally labile fractions, likely through physical protection mechanisms that reduce microbial accessibility (Paul et al., 2006; De Neve & Hofman, 2000). CEC showed a moderate positive effect, consistent with organo-mineral interactions that stabilize organic matter decomposing at higher temperatures. The presence of trace elements, such as Mn and Zn among the predictors, suggests that redox-active elements may influence S_2 dynamics in certain environments, aligning with previous findings on trace metal involvement in SOC stabilization (Hall et al., 2016; Hall & Silver, 2015).

3.3.3. *S3′ Model*

The S_3 model also exhibited strong predictive performance, with a CCC of 0.85 and RMSE of 1.09 mg-CO_2/g-rock (Table 2 and Fig. 5). Variable importance analysis (Fig. 6) identified POXC as the most influential predictor (100%), followed by aggregate stability (61%) and CEC (41%). This indicates that S3', representing CO_2 evolved from oxygen-containing functional groups, is primarily associated with labile organic matter, soil structural properties, and cation exchange capacity. These findings align with previous studies highlighting the rapid turnover and microbial accessibility of labile SOC as primary factors in decomposition and stabilization processes (Gillespie et al., 2014; Gregorich et al., 2015; Haynes, 2005). The importance of aggregate stability is supported by Bronick and Lal (2005), who

https://doi.org/10.5194/egusphere-2026-2849
Preprint. Discussion started: 12 June 2026

demonstrated that soil macro- and micro-aggregates protect SOC from microbial degradation, thereby reducing CO_2 emissions. Similarly, Six et al. (2002) showed that clay minerals and CEC significantly influence SOC stabilization through mineral-organic interactions.

Partial dependence plots (Fig. 7) revealed consistent patterns across the S_3 model: POXC showed a strong positive relationship with predicted values, while BD exhibited a negative trend. Feature interactions in the S_3 model aligned with established frameworks differentiating labile and mineral-associated organic matter pools in soil carbon dynamics (Cotrufo et al., 2013, 2019, 2022; Giannetta et al., 2018; King et al., 2024; Mitchell et al., 2020).

3.3.4. OI Model

The OI model demonstrated moderate performance, with a CCC = 0.44 and an RMSE = 39.37 mg CO_2 /g TOC, explaining approximately 43% of the variance in OI. While the selected predictors contributed to OI estimation, a significant portion of variability remained unexplained. Among the predictors, total organic nitrogen was the most influential, contributing 100%, followed by NO_3 (95%) and Al (76%). This result aligns with previous studies (e.g., Smith et al., 2015; Murphy, 2014), highlighting the challenges of modeling complex soil processes due to soil heterogeneity. The variable importance plot (Fig. 6) further confirmed that organic matter and nutrient indicators, such as TIN, C:N, and DOC, play a crucial role in regulating biochemical transformations and CO_2 release during organic matter decomposition.

Additionally, soil texture and structural properties, including silt, BD, and aggregate stability, may control soil pores and diffusion pathways within the soil matrix, consistent with Dexter (2004). Chemical parameters, such as NO_3, Fe, P_2O_5, Al, Zn, Na, and S, provided insights into soil nutrient status and indirectly affected microbial activity and oxygen dynamics. These findings support earlier reports by Havlin et al. (2013) emphasizing the intricate relationship between soil chemistry and biological activity.

In the PDP plots (Fig. 7) for the OI model, as total organic nitrogen decreased, NO_3 increased until both reached a stable state, underscoring the role of organic matter decomposition and oxidation. The influence of P_2O_5 further suggests a connection to micronutrient availability, consistent with Kirkby et al. (2013). These results indicate that OI is primarily governed by nitrogen- and phosphate-related properties, mineral interactions, and soil texture, all of which influence soil organic matter oxidation and stability. Future improvements to the OI model could incorporate microbial enzymatic and

https://doi.org/10.5194/egusphere-2026-2849
Preprint. Discussion started: 12 June 2026

environmental variables (e.g., drainage) given the significant roles of iron, nitrate, and phosphate predictors.

3.3.5. HI Model

The HI model was developed using the minimum number of predictors: C:N, BD, NH_4, Al, DOC, aggregate stability, P_2O_5, and Na, with a CCC of 0.48 and an RMSE of 39.4 mg HC/g TOC. The CCC of 0.48 for HI models reflects moderate agreement between predicted and observed values. The variable importance plot (Fig. 6) showed that NH_4 was the most important variable, with a 100% relative contribution to predicting HI. This was followed by C:N with 79%, closely marked by P_2O_5 with ~76%, Al with ~57%, BD with ~34%, DOC with ~18%, and Na with ~5%. High HI values indicate less decomposed, hydrogen-rich organic matter, where mineralization can generate NH_4 and limited nitrification allows it to accumulate; thus, NH_4 is more likely a consequence of high-HI than a cause.

The C:N, the next important variable in the predictive model for HI, conforms with studies on SOC biogeochemical processes. For example, a lower C: N ratio indicates higher N availability, which can enhance microbial activity and decomposition of organic matter, potentially driving HI (Wu et al., 2023). HI informs the presence of labile functional groups with corresponding narrow C:N; hence, HI could be influenced by narrow C:N, suggesting that high N content in an SOC may lead to more hydrogen-rich compounds, thus driving HI.

In Fig. 7 for the PDP plots HI model, C:N exhibited a relatively stable trend with minor fluctuations, indicating a minimal effect on the HI index. In contrast, BD showed a stronger relationship with pyrolysis, likely due to its influence on microbial decomposition and organic matter stabilization. NH_4 initially displayed a sharp increase before stabilizing, suggesting its strong influence on thermal stability at the onset, potentially due to its role in raising pyrolysis temperature before stabilizing as hydrogen molecules were fully released. These findings align with Wang et al., (2023), who reported that ammonium perchlorate decomposition emits gases like HCN and CO_2 at high temperatures.

3.3.6. T_{50} *Model*

In the T_{50} model, the CCC values ranged from 0.58 to 0.66 (Table 2 and Fig. 5), where the most significant variable was NH_4, which was followed by aggregate stability at 89% and DOC at 85 %. Al had a moderate importance level of 34 %, while permanganate oxidizable C showed no relationship with

https://doi.org/10.5194/egusphere-2026-2849
Preprint. Discussion started: 12 June 2026

T_{50} estimation. These results suggest that higher levels of dissolved carbon likely lower the temperature at which 50% of SOC degrades because labile dissolved carbon decomposes at lower temperatures, aligning with previous findings that indicate dissolved carbon can be used to predict SOC stability (Nie et al., 2019; Zhang et al., 2019).

Fig. 7 also shows the PDP for the T_{50} model, highlighting the contribution of each predictor in the prediction. As shown, predictors connected with labile carbon pools yielded negative relationships with T_{50}. The predictors associated with more labile carbon pools generally show negative partial dependence, explaining that increases in variables such as DOC, C:N, and NH_4 are linked to lower predicted T_{50} values. In addition, the model predicts that soils with high amounts of labile organic matter tend to exhibit lower temperatures of decomposition, reflecting reduced thermal stability. This finding is also consistent with Hou et al., (2021), who noted that active carbon pools like dissolved C reduce SOM stability in alpine soils due to their susceptibility to microbial degradation. The increasing trend indicates that the presence of Al, likely in the form of reactive oxides, contributes to SOC stability (Gregorich et al., 2015; Schmidt et al., 2011). Further emphasized that SOC stability depends more on mineral protection than on functional groups (Plante et al. (2011).

Table 2. Accuracy metrics of the predictive models of thermal stability indices

Thermal Stability Indices	r^2	Adj.r^2	CCC	RMSE	Bias	MAE
S_1	0.76	0.76	0.85	1.19	– 0.01	0.79
S_2	0.77	0.77	0.86	4.01	0.01	2.78
S_3	0.77	0.77	0.85	1.09	– 0.01	0.78
OI	0.32	0.32	0.44	21.86	0.42	16.52
HI	0.33	0.33	0.48	39.37	0.81	30.57
T_{50}	0.42	0.42	0.58	15.96	– 0.24	11.85

Note: Coefficient of determination (R^2), adjusted coefficient of determination (Adj. R^2), Lin's concordance correlation coefficient (CCC), root mean square error (RMSE), bias, mean absolute error (MAE).

https://doi.org/10.5194/egusphere-2026-2849
Preprint. Discussion started: 12 June 2026

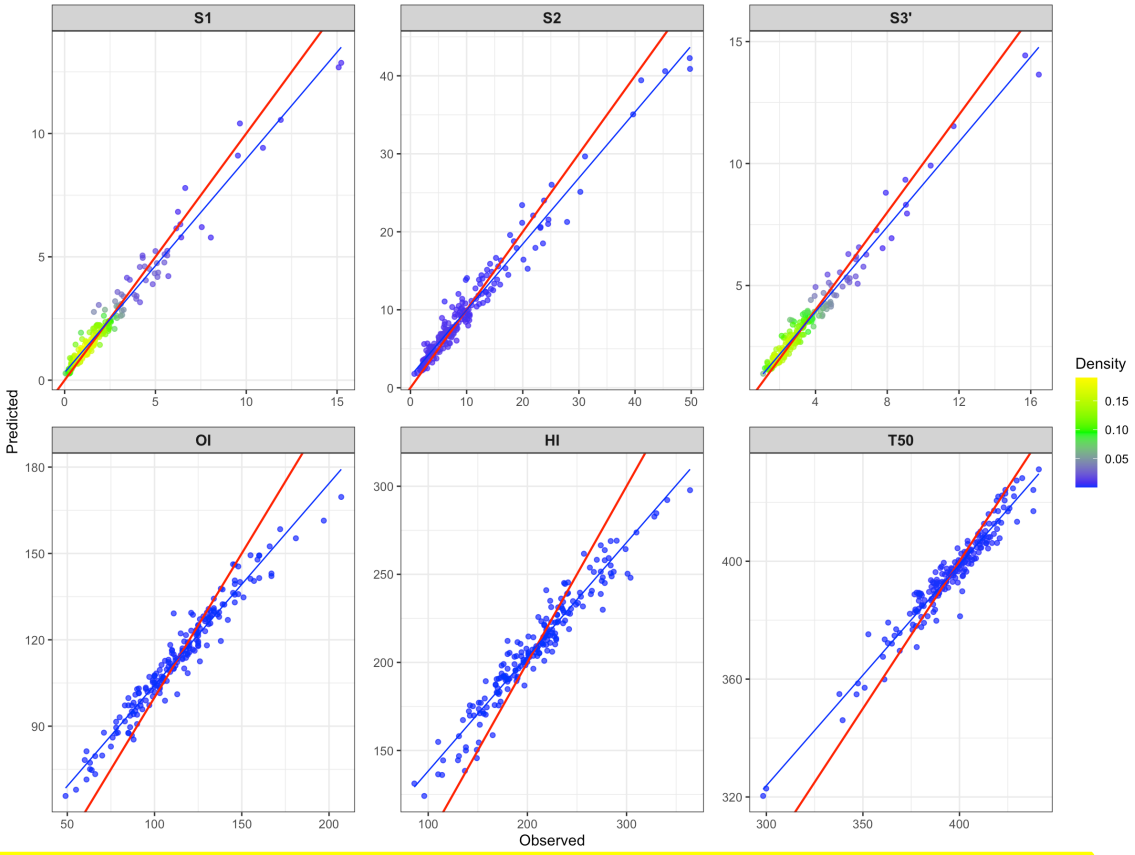

Figure 5. Scatterplot of the predicted versus observed data of the thermal stability indices: S_1 (HC-mg/g-rock), S_2 (HC-mg/g-rock), S3' (mg-CO_2 /g-rock), OI (O_2-mg/g TOC), HI (HC-mg/g TOC), & T_{50} (°C). The red line represents the 1:1 line, and the blue line represents the line of best fit between observed and predicted values.

https://doi.org/10.5194/egusphere-2026-2849
Preprint. Discussion started: 12 June 2026

606

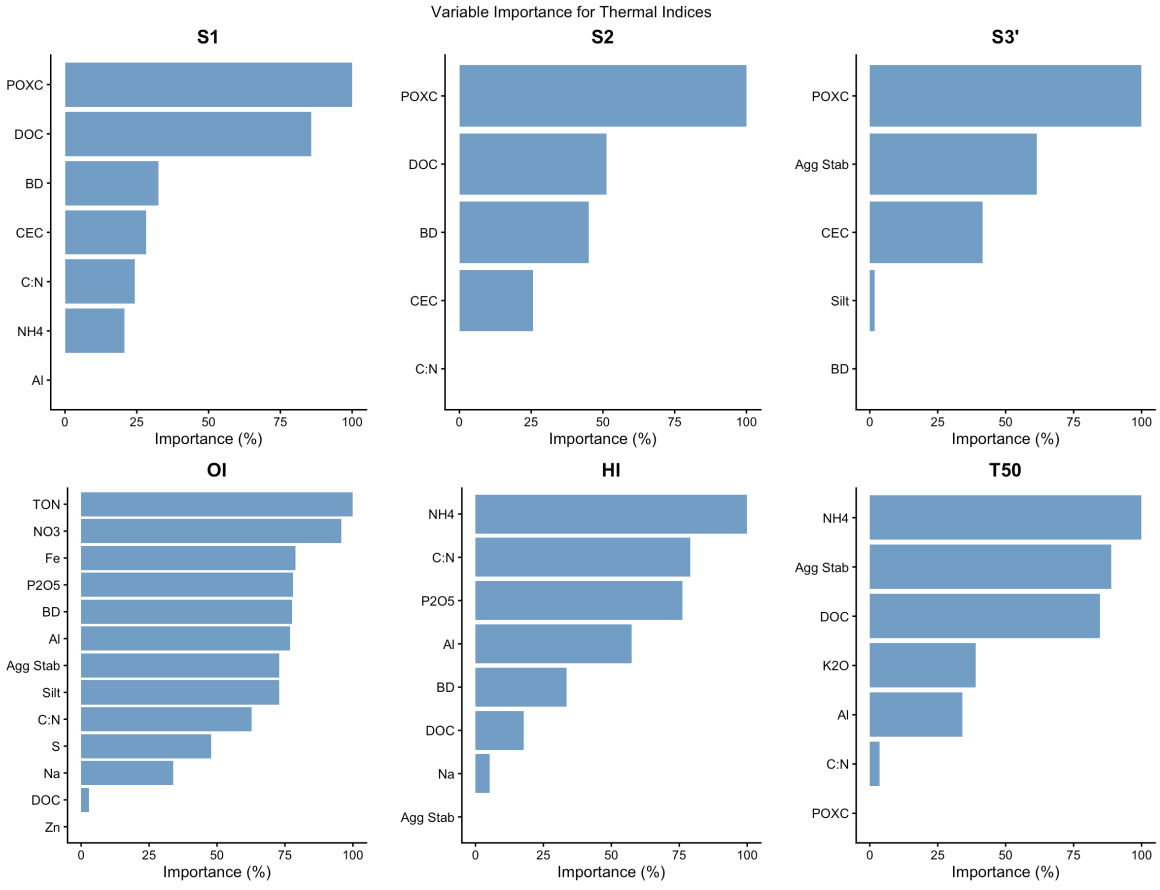

607

608 **Figure 6.** Permutation-based, relative variable importance plots for predicting thermal stability indices
609 using physicochemical properties of soils.

https://doi.org/10.5194/egusphere-2026-2849
Preprint. Discussion started: 12 June 2026

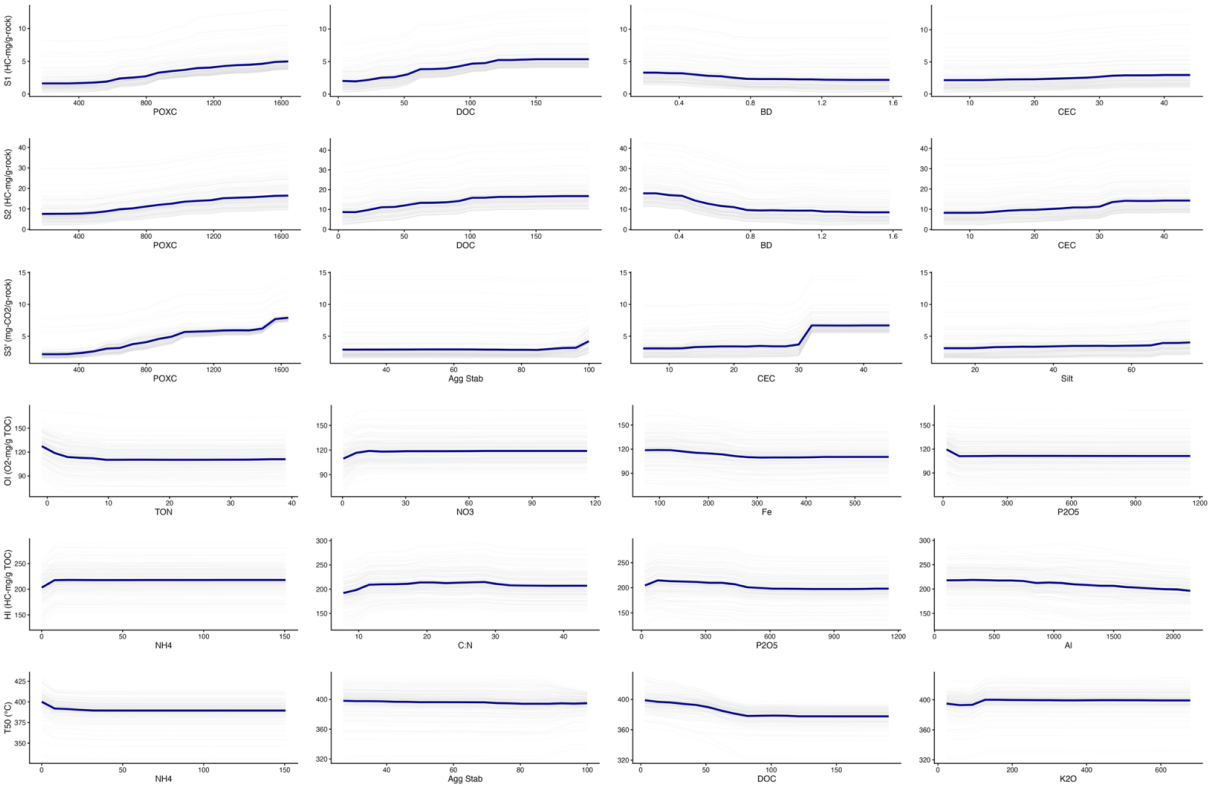

Figure 7. Partial dependence plots generated for the top four most important predictors of thermal stability indices. The grey lines represent the ICE curves, and the blue line represents the average of the Individual Conditional Expectation ICE lines.

3.5. Structural Equation Modelling

We present our SEM as a hypothesis-testing framework that reveals patterns of association rather than demonstrating causation. Our *a priori* model was grounded in soil biogeochemical theory, with individual paths representing hypothesized relationships informed by existing literature (H_1: physical protection, Six et al., 2004; H_2: carbon quality, Lehmann & Kleber, 2015; H_3: pH effects, Rowley et al., 2018; H_4: mineral reactivity, Kleber et al., 2007; H_5: physical structure, Dungait et al., 2012; Tables 3-5 & Fig. 8). Our results demonstrated excellent global fit (CFI = 1.0, RMSEA = 0.0, SRMR < 0.001), satisfying recommended thresholds (CFI ≥ 0.90, RMSEA ≤ 0.08, SRMR ≤ 0.10; Hu & Bentler, 1999; Wade et al., 2026). However, we acknowledge that the saturated nature of our model (df = 0) reflects its simplicity rather than definitive evidence of causal structure.

https://doi.org/10.5194/egusphere-2026-2849
Preprint. Discussion started: 12 June 2026

Our *a priori* hypothesis model explained 53.5% of variance in T_{50}, with cross-validation confirming robustness (10-fold CV with 20 repeats $r^2 = 0.538 \pm 0.03$; CCC = 0.73, 95% CI: 0.68–0.78). Hypothesis testing supported four of five predicted directional relationships: H_1 (clay content showed a significant positive interaction with T_{50}, $\beta = 0.152$, $p = 0.002$), H_2 (DOC; dissolved organic carbon showed a significant negative relationship with T_{50}, $\beta = -0.319$, $p < 0.001$), H_3 (soil pH showed a significant positive relationship with T_{50}, $\beta = 0.436$, $p < 0.001$), and H_4 (Al; aluminum showed a significant positive interaction with T_{50}, $\beta = 0.379$, $p < 0.001$). However, H_5 (bulk density) was not supported ($\beta = 0.057$, $p = 0.305$), indicating that physical structure, as measured by density, may be secondary to chemical factors in its relationship with thermal stability.

We further tested competing configurations using mediation analysis (H6–H7; Fig. 9) and an exploratory model that included POXC, C: N, and P_2O_5. Clay content showed significant indirect interaction via DOC (indirect $\beta = -0.074$, $p = 0.033$), and pH demonstrated indirect associations through both DOC (indirect $\beta = 0.142$, $p = 0.002$) and aluminum (indirect $\beta = -0.113$, $p < 0.001$), with a substantial total association ($\beta = 0.501$, $p < 0.001$). These mediation pathways illustrate the complex interplay among soil properties that simple bivariate correlations cannot capture. However, we caution that temporal precedence, a key criterion for causal inference (Hill, 1965; Wade et al., 2026), cannot be established from our single time-point sampling. Thus, while our results are consistent with the hypothesized directional relationships, they represent interaction evidence that contributes to, but does not definitively establish, causal understanding.

Model robustness was assessed through multiple approaches: (1) bootstrapped standard errors ($n = 1000$) for mediation paths, (2) 10-fold cross-validation (CV) with 20 repeats ($R^2 = 0.538$, RMSE = 17.92 ± 1.2), and (3) examination of residual correlations (all < 0.10, indicating acceptable local fit). The exploratory model incorporating POXC, C:N, and P_2O_5 increased explained variance to 57.2% but reduced parsimony, with only POXC showing a significant association ($\beta = -0.259$, $p < 0.001$). Following Wade et al.'s (2026) guidance on distinguishing confirmatory from exploratory analyses, we present these exploratory findings as hypothesis-generating rather than confirmatory, requiring validation in future studies. Collectively, our results demonstrate that pH, aluminum, and dissolved carbon are primary drivers of SOC thermal stability, with clay playing a complex mediating role. Consistent with Wade et al. (2026), who caution that any single analytical approach cannot confirm causal relationships, we position our findings as one line of correlational evidence contributing to an accumulating knowledge base on SOC stabilization.

https://doi.org/10.5194/egusphere-2026-2849
Preprint. Discussion started: 12 June 2026

Table 3. Standardized path coefficients (β) and bootstrapped standard errors (SE) from SEM showing pathways to SOC thermal stability

Predictors	Std. Coefficient	SE	*p*-Value
	a priori Effects		
pH	0.44	0.06	0.001
Al	0.38	0.06	0.001
DOC	–0.32	0.06	0.001
Clay	0.15	0.05	0.001
BD	0.06	0.06	ns[5]
	Exploratory Effects		
pH	0.46	0.08	0.001
Al	0.36	0.05	0.001
POXC	–0.26	0.08	0.001
Clay	0.16	0.05	0.01
DOC	–0.16	0.07	0.05
C:N	–0.12	0.07	ns[5]
BD	–0.11	0.07	ns[5]
P_2O_5	0.04	0.05	ns[5]

Note: [5]ns = not significant

Table 4. Summary of hypothesis tests evaluating direct and indirect pathways in SEM of SOC thermal stability

Hypothesis	Description	Prediction	Effect Size	*p*-Value	Confirmed
H_1	Clay ~ T_{50} – Physical protection	positive	0.152	0.00	Yes (direction correct)
H_2	DOC ~ T_{50} – Labile carbon	negative	–0.319	0.00	Yes (direction correct)
H_3	pH ~ T_{50} – Acidity	positive	0.436	0.00	Yes (direction correct)
H_4	Al ~ T_{50} – Mineral reactivity	positive	0.379	0.00	Yes (direction correct)
H_5	BD ~ T_{50} – Structure	positive	0.057	0.31	No (not significant)
H_6	Clay indirect effects via DOC and Al	mediation	0.048	0.03	Yes
H_7	pH indirect effects via DOC and Al	mediation	0.241	0.00	Yes

https://doi.org/10.5194/egusphere-2026-2849
Preprint. Discussion started: 12 June 2026

Note: Standardized coefficients represent the strength of association. For mediation hypotheses, coefficients represent the indirect effect magnitude. Supported hypotheses indicate statistical significance ($p < 0.05$) and direction consistent with predictions

Table 5. Goodness-of-fit statistics for confirmatory, exploratory, and mediation SEM predicting SOC thermal stability

Model	Type	[6]AIC	[7]BIC	[8]CFI	[9]RMSEA	R^2
a priori Hypothesis	Confirmatory (theory-driven)	433.51	456.70	1.00	0.00	0.54
Exploratory	Exploratory	422.84	455.97	1.00	0.00	0.57
Mediation	Confirmatory (mediation)	1520.82	1557.27	0.86	0.41	0.49

Note: [6]Lower AIC values indicate better fit; [7]Lower BIC values indicate better fit; [8]CFI ≥ 0.90 acceptable, ≥ 0.95 good fit; [9]RMSEA ≤ 0.08 acceptable, ≤ 0.05 good fit

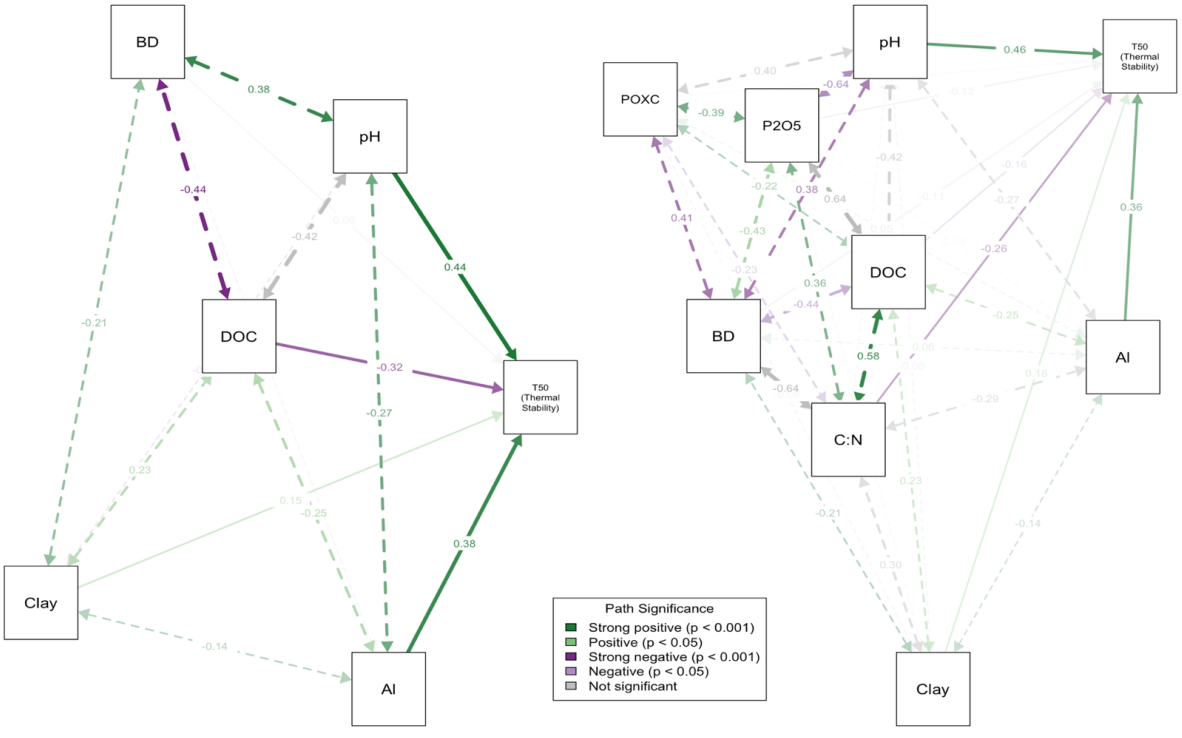

Figure 8. Path diagram from structural equation modeling (SEM) showing the multivariate relationship between soil properties and thermal stability (T_{50}).
Note: Green arrows indicate significant positive relationships ($p < 0.001$, thick; $p < 0.05$, thin); purple arrows indicate significant negative relationships. Values adjacent to arrows are standardized path coefficients, representing the strength of association between variables. The model explains 53.5% of the variance in T_{50} ($R^2 = 0.54$). Solid arrows represent direct effects, while dashed arrows

https://doi.org/10.5194/egusphere-2026-2849
Preprint. Discussion started: 12 June 2026

represent indirect pathways, meaning the predictors influence T_{50} *via* one or more mediators rather than directly.

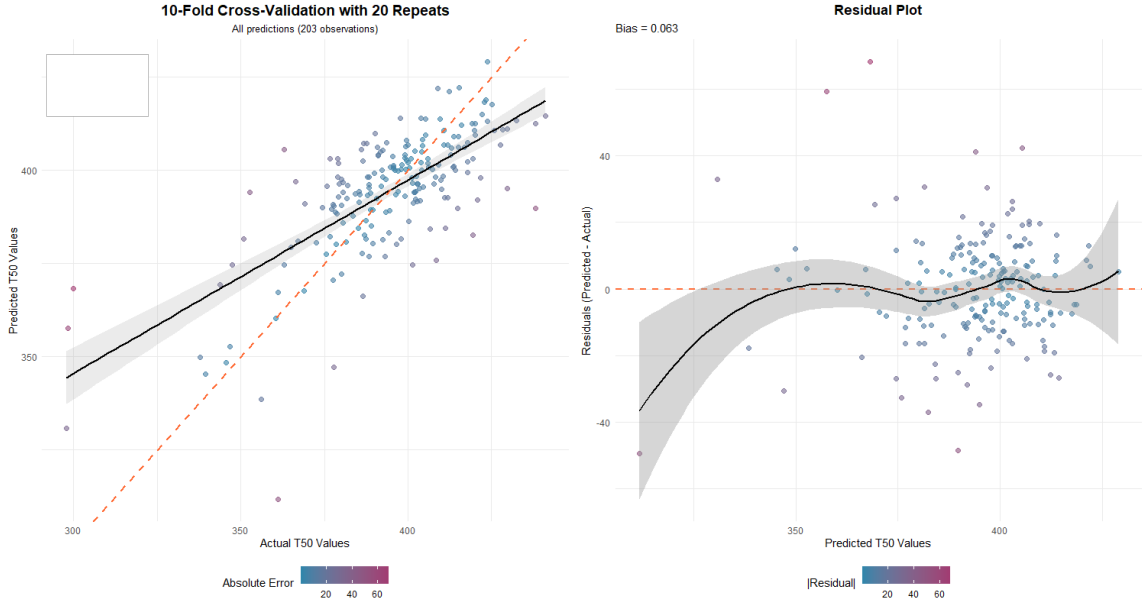

Figure 9. Model performance evaluation for the structural equation model (SEM) predicting thermal stability(T_{50}) using 10-fold cross-validation repeated 20 times (*n* = 203 sample points). Left: 1:1 scatterplot of observed vs. predicted T_{50} values with identity line (solid black), regression fit (gray), and 1:1 dashed reference; points colored by absolute error magnitude. Right: Residual plot (predicted – actual) showing low overall bias (0.063) and minimal systematic patterns across predicted values.

https://doi.org/10.5194/egusphere-2026-2849
Preprint. Discussion started: 12 June 2026

4. CONCLUSIONS

In conclusion, assessing SOC stability is essential for understanding carbon sequestration potential and its response to environmental change. Our analysis of thermal stability indices from HAWK-programmed pyrolysis revealed distinct patterns across land uses. Forest soils showed higher T_{50} with moderate to high S_2, consistent with greater thermal stability and more recalcitrant SOC. Agricultural land use yielded lower and more variable T_{50} with correspondingly high S_1 and HI, suggesting associations with disturbance-driven decomposition and labile carbon pools. Wetlands exhibited high S_2 with variable T_{50}, consistent with fresh organic matter accumulation under anaerobic conditions. Pasture sites showed intermediate values, with moderate T_{50} and HI related to perennial root inputs, grazing, and partial mineral protection.

Using random forest modeling, we identified several soil properties—including bulk density, permanganate oxidizable carbon (POXC), cation exchange capacity (CEC), and nutrient content—that showed strong associations with thermal stability indices. Our findings detail how soil properties relate to SOC stability through organo-mineral interactions, microbial activity, and soil structure. The positive correlation between aluminum and thermal stability indices suggests that Al plays a role in SOC stabilization, reflected in higher thermal decomposition temperatures.

Partial dependence plots (PDP) and individual conditional expectation (ICE) plots revealed nonlinear relationships between key predictors, enhancing our understanding of thermal decomposition patterns across temperature ranges. Additionally, our SEM analysis supported hypothesized directional relationships: clay and pH showed direct positive associations with T_{50}, while dissolved organic carbon showed a direct negative association with T_{50}. Mediation analysis further revealed indirect pathways through which clay and pH relate to T_{50} via dissolved carbon and aluminum. These results demonstrate that HAWK-programmed pyrolysis thermal stability indices are related to measurable soil properties, capturing complex soil interactions and providing insights into SOC stability.

We also identified limitations, particularly the modest predictive performance for OI, suggesting that additional variables (e.g., microbial biomass, enzymatic activity, climate, topography, land use) may better capture SOC oxidation processes. Future research should refine predictive models for lower-performing thermal stability indices using theory-based variables and assess their transferability across regions and soil types. Additionally, we recommend testing hypothesized relationships for other thermal

https://doi.org/10.5194/egusphere-2026-2849
Preprint. Discussion started: 12 June 2026

indicators to further elucidate multivariate associations between soil properties and SOC thermal stability. Further investigation into mineral-organic interactions, particularly in soils with high clay content or reactive minerals, will help clarify their role in SOC stabilization. Addressing these gaps will enhance predictive modeling of thermal indices, providing a framework for monitoring SOC sequestration and stability.

CODE AND DATA AVAILABILITY

Data will be made available upon reasonable request but are not available in any online repository to protect the privacy concerns of the participants in this project.

SUPPLEMENT

The supplementary Tables and Figures related to this article are attached along with the manuscript text

AUTHOR CONTRIBUTIONS

KJ, TP, BH, AWG, LPC, and DHL conceptualized the study. LPC contributed to the design of the soil sampling and analytical framework. KJ, TP, and BH conducted the data analysis and modelling, with input from AWG, MM, LPC, and DHL. KJ prepared the original manuscript draft. All authors contributed to the interpretation of the results, reviewed and edited the manuscript, and approved the final version for submission.

DECLARATION OF COMPETING INTEREST

The authors declare that they have no known competing financial interests or personal relationships that could have appeared to influence the work reported in this paper.

ACKNOWLEDGEMENTS

We are very grateful to all landowners who have given us access to their property to collect soil samples. For soil sample collection and general soil analyses, we would like to thank: Technicians Kyle MacKinley, Karen Terry, Mohammad Islam, and Pam MacKinley; Students Vanessa Mossman, Valentin Nugues, Erika Young, Matthew A.C. Milne, Kayli McGarrigle, Allysia Murphy, Simon Bertheleme, Violet Eliza-Sioux James, and Madison White. The authors recognize funding received through the Sustainable Agriculture Research Initiative Grant (ALLRP 588521-23), supported jointly by the Natural Sciences and Engineering Research Council of Canada (NSERC), the Social Sciences and

https://doi.org/10.5194/egusphere-2026-2849
Preprint. Discussion started: 12 June 2026

Humanities Research Council (SSHRC), and Agriculture and Agri-Food Canada. This research was undertaken, in part, thanks to funding from the Canada Research Chairs Program awarded to Heung.

REFERENCES

Almagro, M., Ruiz-Navarro, A., Díaz-Pereira, E., Albaladejo, J., and Martínez-Mena, M.: Plant residue chemical quality modulates the soil microbial response related to decomposition and soil organic carbon and nitrogen stabilization in a rainfed Mediterranean agroecosystem, Soil Biol. Biochem., 156, 108198, https://doi.org/10.1016/j.soilbio.2021.108198, 2021.

An, Z., Pokharel, P., Plante, A. F., Bork, E. W., Carlyle, C. N., Williams, E. K., & Chang, S. X.: Soil organic matter stability in forest and cropland components of two agroforestry systems in western Canada. *Geoderma*, *433*, 116463, 2023

Apley, D. W., and Zhu, J.: Visualizing the Effects of Predictor Variables in Black Box Supervised Learning Models, J. R. Stat. Soc. Ser. B Stat. Methodol., 82(4), 1059-1086, https://doi.org/10.1111/rssb.12377, 2020.

Arbor, A., Schmidt, M., Saurette, D., Zhang, J., Bulmer, C., Filatow, D., Kasraei, B., Smukler, S., and Heung, B.: A framework for recalibrating pedotransfer functions using nonlinear least squares and estimating uncertainty using quantile regression, Geoderma, 439, 116674, https://doi.org/10.1016/j.geoderma.2023.116674, 2023.

Arbor, A., Schmidt, M., Zhang, J., Bulmer, C., Filatow, D., Kasraei, B., Smukler, S., and Heung, B.: Filling the gaps in soil data: A multi-model framework for addressing data gaps using pedotransfer functions and machine-learning with uncertainty estimates to estimate bulk density, Catena, 245, 108310, https://doi.org/10.1016/j.catena.2024.108310, 2024.

Barreto, M. S. C., Elzinga, E. J., Ramlogan, M., Rouff, A. A., and Alleoni, L. R. F.: Calcium enhances adsorption and thermal stability of organic compounds on soil minerals, Chem. Geol., 559, 119804, https://doi.org/10.1016/j.chemgeo.2020.119804, 2021.

Barreto, M. S. C., Ramlogan, M., Oliveira, D. M. S., Verburg, E. E. J., Elzinga, E. J., Rouff, A. A., Jemo, M., and Alleoni, L. R. F.: Thermal stability of soil organic carbon after long-term manure application across land uses and tillage systems in an oxisol, Catena, 200, 105164, https://doi.org/10.1016/j.catena.2021.105164, 2021.

Barros, N., Salgado, J., Villanueva, M., Rodriquez-Añón, J., Proupin, J., Feijóo, S., and Martín-Pastor, M.: Application of DSC–TG and NMR to study the soil organic matter, J. Therm. Anal. Calorim., 104(1), 53-60, https://doi.org/10.1007/s10973-010-1163-4, 2011.

Barré, P., Cécillon, L., and Kanari, E.: Characterization and Evaluation of the Stability of Soil Organic Matter, The Rock-Eval Method, 181-207, https://doi.org/10.1002/9781394256235.ch10, 2024.

Baudin, F., Disnar, J. R., Aboussou, A., and Savignac, F.: Guidelines for Rock–Eval analysis of recent marine sediments, Org. Geochem., 86, 71-80, https://doi.org/10.1016/j.orggeochem.2015.06.009, 2015.

https://doi.org/10.5194/egusphere-2026-2849
Preprint. Discussion started: 12 June 2026

787 Berthrong, S. T., Jobbágy, E. G., and Jackson, R. B.: A global meta-analysis of soil exchangeable
788 cations, pH, carbon, and nitrogen with afforestation, Ecol. Appl., 19(8), 2228-2241,
789 https://doi.org/10.1890/08-1730.1, 2009.
790 Berthrong, S. T., Piñeiro, G., Jobbágy, E. G., and Jackson, R. B.: Soil C and N changes with
791 afforestation of grasslands across gradients of precipitation and plantation age, Ecol. Appl.,
792 22(1), 76-86, https://doi.org/10.1890/10-2210.1, 2012.
793 Bouma, J.: Using Soil Survey Data for Quantitative Land Evaluation, Advances in Soil Science, 177-
794 213, https://doi.org/10.1007/978-1-4612-3532-3_4, 1989.
795 Breiman, L., Friedman, J. H., Olshen, R. A., and Stone, C. J.: Classification and regression trees,
796 Wadsworth International Group, Belmont, California, 1984.
797 Breiman, L.: Random forests, Machine Learning, 45, 5–32, https://doi.org/10.1023/A:1010933404324,
798 2001.
799 Briedis, C., de Moraes Sá, J. C., Lal, R., de Oliveira Ferreira, A., Franchini, J. C., and Milori, D. M. B.
800 P.: Preservation of labile organic compounds is the pathway for carbon storage in a 23-year
801 continuous no-till system on a Ferralsol in southern Brazil, Geoderma Regional, 33, e00643,
802 https://doi.org/10.1016/j.geodrs.2023.e00643, 2023.
803 Bronick, C., and Lal, R.: Soil structure and management: a review, Geoderma, 124(1-2), 3-22,
804 https://doi.org/10.1016/j.geoderma.2004.03.005, 2005.
805 Casalicchio, G., Molnar, C., and Schratz, P.: iml: Interpretable Machine Learning, CRAN: Contributed
806 Packages, https://doi.org/10.32614/cran.package.iml, 2018.
807 Cécillon, L., Baudin, F., Chenu, C., Houot, S., Jolivet, R., Kätterer, T., Lutfalla, S., Macdonald, A., van
808 Oort, F., Plante, A. F., Savignac, F., Soucémarianadin, L. N., and Barré, P.: A model based on
809 Rock-Eval thermal analysis to quantify the size of the centennially persistent organic carbon
810 pool in temperate soils, Biogeosciences, 15(9), 2835-2849, https://doi.org/10.5194/bg-15-2835-
811 2018, 2018.
812 Cotrufo, M. F., Haddix, M. L., Kroeger, M. E., and Stewart, C. E.: The role of plant input physical-
813 chemical properties, and microbial and soil chemical diversity on the formation of particulate
814 and mineral-associated organic matter, Soil Biol. Biochem., 168, 108648,
815 https://doi.org/10.1016/j.soilbio.2022.108648, 2022.
816 Cotrufo, M. F., Ranalli, M. G., Haddix, M. L., Six, J., and Lugato, E.: Soil carbon storage informed by
817 particulate and mineral-associated organic matter, Nature Geoscience, 12(12), 989-994,
818 https://doi.org/10.1038/s41561-019-0484-6, 2019.
819 Cotrufo, M. F., Wallenstein, M. D., Boot, C. M., Denef, K., and Paul, E.: The Microbial Efficiency-
820 Matrix Stabilization (MEMS) framework integrates plant litter decomposition with soil organic
821 matter stabilization: do labile plant inputs form stable soil organic matter?, Glob. Change Biol.,
822 19(4), 988-995, https://doi.org/10.1111/gcb.12113, 2013.
823 Craney, T. A., and Surles, J. G.: Model-Dependent Variance Inflation Factor Cutoff Values, Quality
824 Engineering, 14(3), 391-403, https://doi.org/10.1081/qen-120001878, 2002.

https://doi.org/10.5194/egusphere-2026-2849
Preprint. Discussion started: 12 June 2026

Cremer, M., and Prietzel, J.: Soil acidity and exchangeable base cation stocks under pure and mixed stands of European beech, Douglas fir and Norway spruce, Plant Soil, 415(1-2), 393-405, https://doi.org/10.1007/s11104-017-3177-1, 2017.

Culman, S. W., Snapp, S. S., Freeman, M. A., Schipanski, M. E., Beniston, J., Lal, R., Drinkwater, L. E., Franzluebbers, A. J., Glover, J. D., Grandy, A. S., Lee, J., Six, J., Maul, J. E., Mirksy, S. B., Spargo, J. T., and Wander, M. M.: Permanganate Oxidizable Carbon Reflects a Processed Soil Fraction that is Sensitive to Management, Soil Sci. Soc. Am. J., 76(2), 494-504, https://doi.org/10.2136/sssaj2011.0286, 2012.

Curto, J. D., and Pinto, J. C.: The corrected VIF (CVIF), Journal of Applied Statistics, 38(7), 1499-1507, https://doi.org/10.1080/02664763.2010.505956, 2011.

da Silva, H. F., de Sousa, P. V. F., Escobar, M. E. O., and de Oliveira, T. S. (2025). Changes in the composition of soil organic matter caused by organic and conventional management in the long term. *Journal of Environmental Management*, *374*, 124018, 2025.

Davidson, E. A., and Janssens, I. A.: Temperature sensitivity of soil carbon decomposition and feedbacks to climate change, Nature, 440(7081), 165-173, https://doi.org/10.1038/nature04514, 2006.

Delahaie, A. A., Barré, P., Baudin, F., Arrouays, D., Bispo, A., Boulonne, L., Chenu, C., Jolivet, C., Martin, M. P., Ratié, C., Saby, N. P. A., Savignac, F., and Cécillon, L.: Elemental stoichiometry and Rock-Eval® thermal stability of organic matter in French topsoils, SOIL, 9(1), 209-229, https://doi.org/10.5194/soil-9-209-2023, 2023.

De Neve, S. and Hofman, G.: Influence of soil compaction on carbon and nitrogen mineralization of soil organic matter and crop residues, Biol. Fertil. Soils, 30, 544–549, https://doi.org/10.1007/s003740050034, 2000.

Dexter, A.R.: Soil physical quality: Part I. Theory, effects of soil texture, density, and organic matter, and effects on root growth. *Geoderma*, *120*(3-4), pp.201-214, 2004

Disnar, J., Guillet, B., Keravis, D., Di-Giovanni, C., and Sebag, D.: Soil organic matter (SOM) characterization by Rock-Eval pyrolysis: scope and limitations, Org. Geochem., 34(3), 327-343, https://doi.org/10.1016/s0146-6380(02)00239-5, 2003.

Doležalová-Weissmannová, H., Malý, S., Brtnický, M., Holátko, J., Demyan, M. S., Siewert, C., Tokarski, D., Kameníková, E., and Kučerík, J.: Practical applications of thermogravimetry in soil science: Part 5. Linking the microbial soil characteristics of grassland and arable soils to thermogravimetry data, J. Therm. Anal. Calorim., 148, 1599–1611, https://doi.org/10.1007/s10973-022-11709-6, 2023.

Dungait, J. A. J., Hopkins, D. W., Gregory, A. S., and Whitmore, A. P.: Soil organic matter turnover is governed by accessibility not recalcitrance, Glob. Change Biol., 18, 1781–1796, https://doi.org/10.1111/j.1365-2486.2012.02665.x, 2012.

Entio, L. J., Taggart, C. B., Muir, J. P., Kan, E., Brady, J. A., and Obayomi, O.: Biochar and Dairy Manure Amendment Effects on Cynodon dactylon Performance and Soil Properties, Plants, 13(2), 242, https://doi.org/10.3390/plants13020242, 2024.

https://doi.org/10.5194/egusphere-2026-2849
Preprint. Discussion started: 12 June 2026

Epskamp, S., Cramer, A. O. J., Waldorp, L. J., Schmittmann, V. D., and Borsboom, D.: qgraph: Network visualizations of relationships in psychometric data, J. Stat. Softw., 48, 1–18, https://doi.org/10.18637/jss.v048.i04, 2012.

Fahmy, S. H., Rees, H. W., Wang, C., and Walker, J. A.: Soil survey reports of New Brunswick, Agriculture and Agri-Food Canada, Fredericton, New Brunswick, 2010.

Fang, K., Chen, L., Qin, S., Zhang, Q., Liu, X., Chen, P., and Yang, Y.: Mineral and Climatic Controls Over Soil Organic Matter Stability Across the Tibetan Alpine Permafrost Region, Global Biogeochemical Cycles, 35(12), e2021GB007118, https://doi.org/10.1029/2021gb007118, 2021.

Fernández, J. M., Peltre, C., Craine, J. M., and Plante, A. F.: Improved Characterization of Soil Organic Matter by Thermal Analysis Using CO₂/H₂O Evolved Gas Analysis, Environmental Science & Technology, 46(16), 8921-8927, https://doi.org/10.1021/es301375d, 2012.

Fernández, J. M., Plante, A. F., Leifeld, J., and Rasmussen, C.: Methodological considerations for using thermal analysis in the characterization of soil organic matter, J. Therm. Anal. Calorim., 104(1), 389-398, https://doi.org/10.1007/s10973-010-1145-6, 2011.

Furze, S. and Arp, P.: Amalgamation and harmonization of soil survey reports into a multi-purpose database. Canadian Journal of Soil Science, 101(2), pp.222-247, 2020

Furze, S., O'Sullivan, A.M., Allard, S., Pronk, T. and Curry, R.A., 2021. A high-resolution, random forest approach to mapping depth-to-bedrock across shallow overburden and post-glacial terrain. Remote Sensing, 13(21), p.4210, 2021

Friedman, J. H.: Greedy function approximation: A gradient boosting machine, The Annals of Statistics, 29(5), https://doi.org/10.1214/aos/1013203451, 2001.

Gao, W., Zhou, T., and Ren, T.: Conversion from Conventional to No Tillage Alters Thermal Stability of Organic Matter in Soil Aggregates, Soil Sci. Soc. Am. J., 79(2), 585-594, https://doi.org/10.2136/sssaj2014.08.0334, 2015.

Giannetta, B., Plaza, C., Vischetti, C., Cotrufo, M. F., and Zaccone, C.: Distribution and thermal stability of physically and chemically protected organic matter fractions in soils across different ecosystems, Biology and Fertility of Soils, 54(5), 671-681, https://doi.org/10.1007/s00374-018-1290-9, 2018.

Gillespie, A., Sanei, H., Diochon, A., Ellert, B., Regier, T., Chevrier, D., Dynes, J., Tarnocai, C., and Gregorich, E.: Perennially and annually frozen soil carbon differ in their susceptibility to decomposition: Analysis of Subarctic earth hummocks by bioassay, XANES and pyrolysis, Soil Biol. Biochem., 68, 106-116, https://doi.org/10.1016/j.soilbio.2013.09.021, 2014.

Goñi, F. M., and Alonso, A.: Differential Scanning Calorimetry in the Study of Lipid Structures, Chemical Biology, 47-66, https://doi.org/10.1002/9780470319253.ch4, 2006.

Goldstein, A., Kapelner, A., Bleich, J., and Pitkin, E.: Peeking Inside the Black Box: Visualizing Statistical Learning With Plots of Individual Conditional Expectation, Journal of Computational and Graphical Statistics, 24(1), 44-65, https://doi.org/10.1080/10618600.2014.907095, 2015.

https://doi.org/10.5194/egusphere-2026-2849
Preprint. Discussion started: 12 June 2026

Grace, J. B., Scheiner, S. M., and Schoolmaster, D. R.: Structural equation modeling, in: Ecological Statistics: Contemporary Theory and Application, edited by: Fox, G. A., Negrete-Yankelevich, S., and Sosa, V. J., Oxford University Press, Oxford, 168–199, https://doi.org/10.1093/acprof:oso/9780199672547.003.0009, 2015.

Gregorich, E., Gillespie, A., Beare, M., Curtin, D., Sanei, H., and Yanni, S.: Evaluating biodegradability of soil organic matter by its thermal stability and chemical composition, Soil Biol. Biochem., 91, 182-191, https://doi.org/10.1016/j.soilbio.2015.08.032, 2015.

Hall, S. J., and Silver, W. L.: Reducing conditions, reactive metals, and their interactions can explain spatial patterns of surface soil carbon in a humid tropical forest, Biogeochemistry, 125(2), 149-165, https://doi.org/10.1007/s10533-015-0120-5, 2015.

Hall, S. J., Silver, W. L., Timokhin, V. I., and Hammel, K. E.: Iron addition to soil specifically stabilized lignin, Soil Biol. Biochem., 98, 95-98, https://doi.org/10.1016/j.soilbio.2016.04.010, 2016.

Haynes, R.: Labile Organic Matter Fractions as Central Components of the Quality of Agricultural Soils: An Overview, Advances in Agronomy, 221-268, https://doi.org/10.1016/s0065-2113(04)85005-3, 2005.

Hill, A. B.: The environment and disease: association or causation?, Proc. R. Soc. Med., 58, 295–300, 1965.

Hu, L. and Bentler, P. M.: Cutoff criteria for fit indexes in covariance structure analysis: conventional criteria versus new alternatives, Struct. Equ. Modeling, 6, 1–55, https://doi.org/10.1080/10705519909540118, 1999.

IUSS Working Group WRB: World Reference Base for Soil Resources 2006, first update 2007, World Soil Resources Reports, 103, FAO, Rome, 2007.

Kasraei, B., Schmidt, M. G., Zhang, J., Bulmer, C. E., Filatow, D. S., Arbor, A., Pennell, T., and Heung, B.: A framework for optimizing environmental covariates to support model interpretability in digital soil mapping, Geoderma, 445, 116873, https://doi.org/10.1016/j.geoderma.2024.116873, 2024.

Kögel-Knabner, I.: The macromolecular organic composition of plant and microbial residues as inputs to soil organic matter, Soil Biol. Biochem., 34(2), 139-162, https://doi.org/10.1016/s0038-0717(01)00158-4, 2002.

King, A. E., Amsili, J. P., Córdova, S. C., Culman, S., Fonte, S. J., Kotcon, J., Masters, M. D., McVay, K., Olk, D. C., Prairie, A. M., Schipanski, M., Schneider, S. K., Stewart, C. E., and Cotrufo, M. F.: Constraints on mineral-associated and particulate organic carbon response to regenerative management: carbon inputs and saturation deficit, Soil and Tillage Research, 238, 106008, https://doi.org/10.1016/j.still.2024.106008, 2024.

Kirkby, C. A., Richardson, A. E., Wade, L. J., Batten, G. D., Blanchard, C., and Kirkegaard, J. A.: Carbon-nutrient stoichiometry to increase soil carbon sequestration, Soil Biol. Biochem., 60, 77-86, https://doi.org/10.1016/j.soilbio.2013.01.011, 2013.

https://doi.org/10.5194/egusphere-2026-2849
Preprint. Discussion started: 12 June 2026

Kleber, M., Sollins, P., and Sutton, R.: A conceptual model of organo-mineral interactions in soils: self-assembly of organic molecular fragments into zonal structures on mineral surfaces, Biogeochemistry, 85, 9–24, https://doi.org/10.1007/s10533-007-9103-5, 2007.

Kučerík, J., Tokarski, D., Demyan, M. S., Merbach, I., and Siewert, C.: Linking soil organic matter thermal stability with contents of clay, bound water, organic carbon and nitrogen, Geoderma, 316, 38-46, https://doi.org/10.1016/j.geoderma.2017.12.001, 2018.

Kučerík, J., Čtvrtníčková, A., and Siewert, C.: Practical application of thermogravimetry in soil science, J. Therm. Anal. Calorim., 113(3), 1103-1111, https://doi.org/10.1007/s10973-012-2849-6, 2013.

Kuhn, M.: caret: Classification and Regression Training, CRAN: Contributed Packages, https://doi.org/10.32614/cran.package.caret, 2007.

Lal, R.: Soil Carbon Sequestration Impacts on Global Climate Change and Food Security, Science, 304(5677), 1623-1627, https://doi.org/10.1126/science.1097396, 2004.

Laurence, L., Heung, B., Strom, H., Stiles, K., and Burton, D.: Towards a cost-effective framework for estimating soil nitrogen pools using pedotransfer functions and machine learning, Geoderma, 440, 116692, https://doi.org/10.1016/j.geoderma.2023.116692, 2023.

Laurence, L., Heung, B., Zhang, J., Pennell, T., Nyiraneza, J., Strom, H., Stiles, K., and Burton, D. L.: Integrating multi-year crop inventories as a proxy for soil management within a digital soil mapping framework for predicting nitrogen indices, Geoderma, 448, 116944, https://doi.org/10.1016/j.geoderma.2024.116944, 2024.

Lehmann, J., and Kleber, M.: The contentious nature of soil organic matter, Nature, 528(7580), 60-68, https://doi.org/10.1038/nature16069, 2015.

Leifeld, J., Siebert, S., and Kögel-Knabner, I.: Changes in the chemical composition of soil organic matter after application of compost, Eur. J. Soil Sci., 53(2), 299-309, https://doi.org/10.1046/j.1351-0754.2002.00453.x, 2002.

Li, F., Gui, X., Ji, W., and Zhou, C.: Effect of calcium dihydrogen phosphate addition on carbon retention and stability of biochars derived from cellulose, hemicellulose, and lignin, Chemosphere, 251, 126335, https://doi.org/10.1016/j.chemosphere.2020.126335, 2020.

Liu, M., Qiao, N., Xu, X., Fang, H., Wang, H., and Kuzyakov, Y.: C:N stoichiometry of stable and labile organic compounds determine priming patterns, Geoderma, 362, 114122, https://doi.org/10.1016/j.geoderma.2019.114122, 2020.

Li, Z., Xiao, L., Deng, C., Yuan, Z., Liang, C., Xiong, Q., Li, Z., and Nie, X.: Thermal stability of soil organic carbon subjected to water erosion as a function of edaphic factors, Int. J. Sediment Res., 37(1), 26-36, https://doi.org/10.1016/j.ijsrc.2021.06.002, 2022.

Lorenz, M., Maskow, T., and Thiele-Bruhn, S.: Energy stored in soil organic matter is influenced by litter quality and the degree of transformation – A combustion calorimetry study, Geoderma, 443, 116846, https://doi.org/10.1016/j.geoderma.2024.116846, 2024.

Ma, D., He, Z., Zhao, W., Li, R., Sun, W., Wang, W., Lin, P., Wei, L., and Ju, W.: Long-term effects of conventional cultivation on soil cation exchange capacity and base saturation in an arid

https://doi.org/10.5194/egusphere-2026-2849
Preprint. Discussion started: 12 June 2026

desert region, Sci. Total Environ., 949, 175075, https://doi.org/10.1016/j.scitotenv.2024.175075, 2024.

Mayer, M., Leifeld, J., Szidat, S., Mäder, P., Krause, H. M., and Steffens, M.: Dynamic stability of mineral-associated organic matter: enhanced stability and turnover through organic fertilization in a temperate agricultural topsoil, Soil Biol. Biochem., 184, 109095, https://doi.org/10.1016/j.soilbio.2023.109095, 2023.

McElhaney, R. N.: The use of differential scanning calorimetry and differential thermal analysis in studies of model and biological membranes, Chemistry and Physics of Lipids, 30(2-3), 229-259, https://doi.org/10.1016/0009-3084(82)90053-6, 1982.

Mesgar, M., Voroney, R. P., Lo, A., Ardakani, O. H., and Gillespie, A. W.: Chemical composition and thermal stability of topsoil organic carbon: Influence of cropping system and tillage practices, Eur. J. Soil Sci., 75(1), e13459, https://doi.org/10.1111/ejss.13459, 2024.

Minasny, B., and Mcbratney, A. B.: The Neuro-m Method for Fitting Neural Network Parametric Pedotransfer Functions, Soil Sci. Soc. Am. J., 66(4), https://doi.org/10.2136/sssaj2002.1407a, 2002.

Mitchell, E., Scheer, C., Rowlings, D., Cotrufo, M. F., Conant, R. T., Friedl, J., and Grace, P.: Trade-off between 'new' SOC stabilisation from above-ground inputs and priming of native C as determined by soil type and residue placement, Biogeochemistry, 149(2), 221-236, https://doi.org/10.1007/s10533-020-00675-6, 2020.

Moore, P., Lukenbach, M., Kettridge, N., Petrone, R., Devito, K., and Waddington, J.: Peatland water repellency: Importance of soil water content, moss species, and burn severity, Journal of Hydrology, 554, 656-665, https://doi.org/10.1016/j.jhydrol.2017.09.036, 2017.

Murphy, B. W.: Soil Organic Matter and Soil Function – Review of the Literature and Underlying Data, Department of the Environment, Canberra, Australia, 2014.

Nie, X., Yuan, Z., Huang, B., Liao, Y., Zhang, X., Li, Z., and Li, D.: Effects of water erosion on soil organic carbon stability in the subtropical China, Journal of Soils and Sediments, 19(10), 3564-3575, https://doi.org/10.1007/s11368-019-02305-7, 2019.

Padarian, J., Minasny, B., and McBratney, A. B.: Machine learning and soil sciences: a review aided by machine learning tools, SOIL, 6(1), 35-52, https://doi.org/10.5194/soil-6-35-2020, 2020.

Paul, E. A., Morris, S. J., Conant, R. T., and Plante, A. F.: Does the Acid Hydrolysis–Incubation Method Measure Meaningful Soil Organic Carbon Pools?, Soil Sci. Soc. Am. J., 70(3), 1023-1035, https://doi.org/10.2136/sssaj2005.0103, 2006.

Paul, S. S., Heung, B., and Lynch, D. H.: Modeling of total and active organic carbon dynamics in agricultural soil using digital soil mapping: a case study from Central Nova Scotia, Canadian Journal of Soil Science, 103(1), 64-80, https://doi.org/10.1139/cjss-2022-0012, 2023.

Peltre, C., Fernández, J. M., Craine, J. M., and Plante, A. F.: Relationships between Biological and Thermal Indices of Soil Organic Matter Stability Differ with Soil Organic Carbon Level, Soil Sci. Soc. Am. J., 77(6), 2020-2028, https://doi.org/10.2136/sssaj2013.02.0081, 2013.

Plante, A. F., Fernández, J. M., and Leifeld, J.: Application of thermal analysis techniques in soil science, Geoderma, 153(1-2), 1-10, https://doi.org/10.1016/j.geoderma.2009.08.016, 2009.

https://doi.org/10.5194/egusphere-2026-2849
Preprint. Discussion started: 12 June 2026

Plante, A. F., Fernández, J. M., Haddix, M. L., Steinweg, J. M., and Conant, R. T.: Biological, chemical and thermal indices of soil organic matter stability in four grassland soils, Soil Biol. Biochem., 43(5), 1051-1058, https://doi.org/10.1016/j.soilbio.2011.01.024, 2011.

Preacher, K. J. and Hayes, A. F.: Asymptotic and resampling strategies for assessing and comparing indirect effects in multiple mediator models, Behav. Res. Methods, 40, 879–891, https://doi.org/10.3758/BRM.40.3.879, 2008.

Pronk, A. G. and Ruitenberg, A. A.: Bedrock geology of New Brunswick, New Brunswick Department of Natural Resources and Energy, Minerals and Energy Division, Map NR-1, scale 1:500000, 1991.

Rakhsh, F., Golchin, A., Beheshti Al Agha, A., and Alamdari, P.: Effects of exchangeable cations, mineralogy and clay content on the mineralization of plant residue carbon, Geoderma, 307, 150-158, https://doi.org/10.1016/j.geoderma.2017.07.010, 2017.

Rampton, V. N.: Generalized surficial geology map of New Brunswick, Geological Survey of Canada, Map 1594A, scale 1:500000, 1984.

Rasmussen, C., Heckman, K., Wieder, W. R., Keiluweit, M., Lawrence, C. R., Berhe, A. A., Blankinship, J. C., Crow, S. E., Druhan, J. L., Hicks Pries, C. E., Marin-Spiotta, E., Plante, A. F., Schädel, C., Schimel, J. P., Sierra, C. A., Thompson, A., and Wagai, R.: Beyond clay: towards an improved set of variables for predicting soil organic matter content, Biogeochemistry, 137, 297–306, https://doi.org/10.1007/s10533-018-0424-3, 2018.

Risoluti, R., Gullifa, G., Barone, L., Papa, E., and Materazzi, S.: On-Line Thermally Induced Evolved Gas Analysis: An Update—Part 1: EGA-MS, Molecules, 27(11), 3518, https://doi.org/10.3390/molecules27113518, 2022.

Rombolà, A. G., Fabbri, D., Meredith, W., Snape, C. E., and Dieguez-Alonso, A.: Molecular characterization of the thermally labile fraction of biochar by hydropyrolysis and pyrolysis-GC/MS, J. Anal. Appl. Pyrol., 121, 230–239, https://doi.org/10.1016/j.jaap.2016.08.003, 2016.

Rosseel, Y.: lavaan: An R Package for Structural Equation Modeling, J. Stat. Softw., 48(2), https://doi.org/10.18637/jss.v048.i02, 2012.

Rowley, M. C., Grand, S., and Verrecchia, É. P.: Calcium-mediated stabilisation of soil organic carbon, Biogeochemistry, 137, 27–49, https://doi.org/10.1007/s10533-017-0410-1, 2018.

Saurette, D. D.: onsoilsurvey: Making PDSM in Ontario Better, Ontario Ministry of Agriculture, Food and Rural Affairs (OMAFRA), Guelph, Ontario, Canada, 2021.

Schmidt, M. W. I., Torn, M. S., Abiven, S., Dittmar, T., Guggenberger, G., Janssens, I. A., Kleber, M., Kögel-Knabner, I., Lehmann, J., Manning, D. A. C., Nannipieri, P., Rasse, D. P., Weiner, S., and Trumbore, S. E.: Persistence of soil organic matter as an ecosystem property, Nature, 478(7367), 49-56, https://doi.org/10.1038/nature10386, 2011.

Sebag, D., Verrecchia, E., Cécillon, L., Adatte, T., Albrecht, R., Aubert, M., Bureau, F., Cailleau, G., Copard, Y., Decaens, T., Disnar, J. R., Hetényi, M., Nyilas, T., and Trombino, L.: Dynamics of soil organic matter based on new Rock-Eval indices, Geoderma, 284, 185-203, https://doi.org/10.1016/j.geoderma.2016.08.025, 2016.

https://doi.org/10.5194/egusphere-2026-2849
Preprint. Discussion started: 12 June 2026

Shi, D., Lee, T., and Maydeu-Olivares, A.: Understanding the Model Size Effect on SEM Fit Indices, Educational and Psychological Measurement, 79(2), 310-334, https://doi.org/10.1177/0013164418783530, 2019.

Shi, J., Lv, J., Peng, Y., Yao, Y., Wei, X., and Wang, X.: Mechanisms controlling the stability and sequestration of mineral associated organic carbon upon erosion and deposition, Catena, 242, 108119, https://doi.org/10.1016/j.catena.2024.108119, 2024.

Shipley, B.: Cause and correlation in biology: a user's guide to path analysis, structural equations and causal inference with R, 2nd edn., Cambridge University Press, Cambridge, https://doi.org/10.1017/CBO9781139979573, 2016.

Six, J., and Paustian, K.: Aggregate-associated soil organic matter as an ecosystem property and a measurement tool, Soil Biol. Biochem., 68, A4-A9, https://doi.org/10.1016/j.soilbio.2013.06.014, 2014.

Six, J., Bossuyt, H., Degryze, S., and Denef, K.: A history of research on the link between (micro)aggregates, soil biota, and soil organic matter dynamics, Soil and Tillage Research, 79(1), 7-31, https://doi.org/10.1016/j.still.2004.03.008, 2004.

Six, J., Conant, R. T., Paul, E. A., and Paustian, K.: Stabilization mechanisms of soil organic matter: Implications for C-saturation of soils, Plant Soil, 241(2), 155-176, https://doi.org/10.1023/a:1016125726789, 2002.

Solomon, D., Lehmann, J., Harden, J., Wang, J., Kinyangi, J., Heymann, K., Karunakaran, C., Lu, Y., Wirick, S., and Jacobsen, C.: Micro- and nano-environments of carbon sequestration: Multi-element STXM–NEXAFS spectromicroscopy assessment of microbial carbon and mineral associations, Chem. Geol., 329, 53-73, https://doi.org/10.1016/j.chemgeo.2012.02.002, 2012.

Sparks, D. L.: Chemistry of soil organic matter, Environmental Soil Chemistry, 53-80, https://doi.org/10.1016/b978-0-12-656445-7.50007-3, 1995.

Smith, P., Cotrufo, M. F., Rumpel, C., Paustian, K., Kuikman, P. J., Elliott, J. A., McDowell, R., Griffiths, R. I., Asakawa, S., Bustamante, M., House, J. I., Sobocká, J., Harper, R., Pan, G., West, P. C., Gerber, J. S., Clark, J. M., Adhya, T., Scholes, R. J., and Scholes, M. C.: Biogeochemical cycles and biodiversity as key drivers of ecosystem services provided by soils, SOIL, 1, 665–685, https://doi.org/10.5194/soil-1-665-2015, 2015.

Tao, F., Huang, Y., Hungate, B. A., Manzoni, S., Frey, S. D., Schmidt, M. W. I., Reichstein, M., Carvalhais, N., Ciais, P., Jiang, L., Lehmann, J., Wang, Y. P., Houlton, B. Z., Ahrens, B., Mishra, U., Hugelius, G., Hocking, T. D., Lu, X., Shi, Z., Viatkin, K., Vargas, R., Yigini, Y., Omuto, C., Malik, A. A., Peralta, G., Cuevas-Corona, R., Di Paolo, L. E., Luotto, I., Liao, C., Liang, Y. S., Saynes, V. S., Huang, X., and Luo, Y.: Microbial carbon use efficiency promotes global soil carbon storage, Nature, 618(7967), 981-985, https://doi.org/10.1038/s41586-023-06042-3, 2023.

Thompson, C. G., Kim, R. S., Aloe, A. M., and Becker, B. J.: Extracting the Variance Inflation Factor and Other Multicollinearity Diagnostics from Typical Regression Results, Basic and Applied Social Psychology, 39(2), 81-90, https://doi.org/10.1080/01973533.2016.1277529, 2017.

https://doi.org/10.5194/egusphere-2026-2849
Preprint. Discussion started: 12 June 2026

Tisdale, S. L., and Nelson, W. L.: Soil Fertility and Fertilizers, Soil Science, 101(4), 346, https://doi.org/10.1097/00010694-196604000-00016, 1966.

Vallotton, J. D., Comeau, L. P., Goyer, C., Wagg, C., and Unc, A.: Land use is reliably predicted by soil burst respiration profiles, Appl. Soil Ecol., 214, 106315, doi.org, 2025.

Van Looy, K., Bouma, J., Herbst, M., Koestel, J., Minasny, B., Mishra, U., Montzka, C., Nemes, A., Pachepsky, Y. A., Padarian, J., Schaap, M. G., Tóth, B., Verhoef, A., Vanderborght, J., van der Ploeg, M. J., Weihermüller, L., Zacharias, S., Zhang, Y., and Vereecken, H.: Pedotransfer Functions in Earth System Science: Challenges and Perspectives, Reviews of Geophysics, 55(4), 1199-1256, https://doi.org/10.1002/2017rg000581, 2017.

Verchovsky, A., Anand, M., Barber, S., Sheridan, S., and Morgan, G.: A quantitative evolved gas analysis for extra-terrestrial samples, Planetary and Space Science, 181, 104830, https://doi.org/10.1016/j.pss.2019.104830, 2020.

Wade, J., Potter, T. S., and Margenot, A. J.: Commentary: Structural equation models and causal claims in soil science and biogeochemistry – An equation-free "how to", Geoderma, 466, 117702, https://doi.org/10.1016/j.geoderma.2026.117702, 2026.

Wadoux, A. M. C., and Molnar, C.: Beyond prediction: methods for interpreting complex models of soil variation, Geoderma, 422, 115953, https://doi.org/10.1016/j.geoderma.2022.115953, 2022.

Wagai, R., and Mayer, L. M.: Sorptive stabilization of organic matter in soils by hydrous iron oxides, Geochimica et Cosmochimica Acta, 71(1), 25-35, https://doi.org/10.1016/j.gca.2006.08.047, 2007.

Wenyika, P., Enesi, R. O., Gorim, L. Y., and Dyck, M.: Effects of liming on soil biota and related processes in agroecosystems: a review, Discover Soil, 2(1), 37, https://doi.org/10.1007/s44378-025-00063-2, 2025.

Wiesmeier, M., Urbanski, L., Hobley, E., Lang, B., von Lützow, M., Marin-Spiotta, E., van Wesemael, B., Rabot, E., Ließ, M., Garcia-Franco, N., Wollschläger, U., Vogel, H. J., and Kögel-Knabner, I.: Soil organic carbon storage as a key function of soils - A review of drivers and indicators at various scales, Geoderma, 333, 149-162, https://doi.org/10.1016/j.geoderma.2018.07.026, 2019.

Wu, G., Gao, J., Li, H., Ren, F., Liang, D., and Li, X.: Shifts in plant and soil C, N, and P concentrations and C:N:P stoichiometry associated with environmental factors in alpine marshy wetlands in West China, Catena, 221, 106801, https://doi.org/10.1016/j.catena.2022.106801, 2023.

Yu, G. H., Chen, C. M., He, X. H., Zhang, X. Z., and Li, L. N.: Unexpected bulk density and microstructures response to long-term pig manure application in a Ferralic Cambisol Soil: Implications for rebuilding a healthy soil, Soil and Tillage Research, 203, 104668, https://doi.org/10.1016/j.still.2020.104668, 2020.

Zhang, X., Li, Z., Nie, X., Huang, M., Wang, D., Xiao, H., Liu, C., Peng, H., Jiang, J., and Zeng, G.: The role of dissolved organic matter in soil organic carbon stability under water erosion, Ecological Indicators, 102, 724-733, https://doi.org/10.1016/j.ecolind.2019.03.038, 2019.

https://doi.org/10.5194/egusphere-2026-2849
Preprint. Discussion started: 12 June 2026

1139
1140
1141
1142
1143
1144
1145
1146
1147
1148
1149